

Changes in Coordination of Sterically Demanding Hybrid Imidazolylphosphine Ligands on Pd(0) and Pd(II)

Douglas B. Grotjahn,^{*,†} Yi Gong,[†] Lev Zakharov,[‡] James A. Golen,[§] and Arnold L. Rheingold[‡]

Contribution from the Department of Chemistry and Biochemistry, 5500 Campanile Drive, San Diego State University, San Diego, California 92182-1030, and Department of Chemistry and Biochemistry, University of California, San Diego, La Jolla, California 92093-0385

Received July 16, 2005; E-mail: grotjahn@chemistry.sdsu.edu

Abstract: Low-coordinate organometallic complexes are important in structure and catalysis, and hemilability or secondary interactions such as hydrogen bonding enabled by hybrid ligands are receiving increasing attention. To study the factors controlling these phenomena, three new imidazol-2-ylphosphine ligands, **L**, were made. In these ligands, the bulk around P and the hindrance at the basic and potentially coordinating imidazole N-3 were varied. Remarkably, $L_2Pd(0)$ complexes **3a–c** were shown to be two-coordinate, 12-electron species, despite the availability of imidazole N-3 to enter into η^2 -P,N chelation. In oxidative additions of C–X bonds to the Pd(0) complexes, reaction rates and products could be controlled by the nature of the C and X groups and the R groups on the phosphine. Most significantly, whereas **4c-PhI** and **4c-MeOTf** from **3c** are normal *trans*-bis(phosphine)Pd(R)(X) species, **5a-PhI**, **5a-PhBr**, and **5b-PhI** from **3a** and **3b** were shown by X-ray diffraction to be a monomeric species with a single η^2 -P,N-chelating phosphine. From **3a** and methyl triflate, an ionic complex $[6a-Me]^+[OTf]^-$ with one chelating and one nonchelating phosphine was formed, with temperature-dependent windshield-wiper exchange of the two, showing hemilability. Thus, large phosphine substituents (R = *tert*-butyl rather than isopropyl) favor chelation. The chelate Pd–imidazole N-3 bond is longer when the heterocyclic nitrogen is hindered by an adjacent *tert*-butyl group at C-4 (comparing **5a-PhI** and **5b-PhI**). Finally, whereas in $[8b-Ph]^+[OTf]^-$ from **5b-PhI** and isopropylamine, the amine coordinates without chelate opening or hydrogen bonding, in $[10c-Me]^+[OTf]^-$ made from **4c-MeOTf** and isopropylamine, the amine is not only coordinated at N but also donates a hydrogen bond to each phosphine imidazol-2-yl substituent.

Introduction

Catalysis by organometallic complexes invariably involves ligand exchange and transformations.^{1,2} Thus, it is not surprising that in the development of organometallic chemistry, an increasingly important role has been played by two special types of complexes, low-coordinate^{3,4} and hemilabile species,^{5–13} because such complexes readily undergo ligand association or exchange and can show exceptional reactivity and importance in catalytic chemistry.

There are textbook examples of the significance of low-coordinate species: although the ability of Wilkinson's catalyst $CIRh(PPh_3)_3$ (an isolable 16-electron complex) to catalyze the hydrogenation of alkenes was discovered in 1965,^{14,15} it was not until 8 years later that it was appreciated that the even more unsaturated 14-electron species $CIRh(PPh_3)_2$ played an important role in the catalysis, being 10,000 times more reactive than its 16-electron precursor toward oxidative addition of hydrogen.¹⁶ Similarly, for more than 20 years, $Pd(PPh_3)_4$ has been known as a catalyst for reactions involving the activation of carbon–halogen bonds in aryl substrates and coupling of the carbon with other atoms (e. g., Heck and Suzuki¹⁷ reactions). However, in the past 10 years, using sterically demanding and electron-rich phosphines which are proposed to favor formation of low-coordinate catalytic intermediates,^{18,19} the scope of the Suzuki reaction has been remarkably extended to include aryl chlo-

[†] San Diego State University.

[‡] University of California, San Diego.

[§] University of Delaware.

- (1) Collman, J. P.; Hegedus, L. S.; Norton, J. R.; Finke, R. G. *Principles and Applications of Organotransition Metal Chemistry*; University Science Books: Mill Valley, CA, 1987.
- (2) Crabtree, R. H. *The Organometallic Chemistry of the Transition Metals*, 3rd ed.; Wiley: New York, 2000.
- (3) Cummins, C. C. *Prog. Inorg. Chem.* **1998**, *47*, 685–836.
- (4) Cummins, C. C. *Chem. Commun.* **1998**, 1777–1786.
- (5) Braunstein, P.; Naud, F. *Angew. Chem., Int. Ed.* **2001**, *40*, 680–699.
- (6) Börner, A. *Eur. J. Inorg. Chem.* **2001**, 327–337.
- (7) Schneider, J. J. *Nachr. Chem.* **2000**, *48*, 614–616, 618–620.
- (8) Müller, C.; Vos, D.; Jutzi, P. *J. Organomet. Chem.* **2000**, *600*, 127–143.
- (9) Slone, C. S.; Weinberger, D. A.; Mirkin, C. A. *Prog. Inorg. Chem.* **1999**, *48*, 233–350.
- (10) Bader, A.; Lindner, E. *Coord. Chem. Rev.* **1991**, *108*, 27–110.
- (11) Jeffrey, J. C.; Rauchfuss, T. B. *Inorg. Chem.* **1979**, *18*, 2658–2666.
- (12) Okuda, J. *Comments Inorg. Chem.* **1994**, *16*, 185–205.
- (13) Werner, H. *Dalton Trans.* **2003**, 3829–3837.

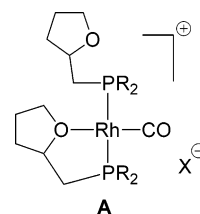
- (14) Young, J. F.; Osborn, J. A.; Jardine, F. H.; Wilkinson, G. *J. Chem. Soc., Chem. Commun.* **1965**, 131–132.
- (15) Osborn, J. A.; Jardine, F. H.; Young, J. F.; Wilkinson, G. *J. Chem. Soc., Dalton Trans.* **1966**, 1711–1732.
- (16) Halpern, J.; Wong, C. S. *J. Chem. Soc., Chem. Commun.* **1973**, 629–630.
- (17) Miyaura, N.; Yanagi, T.; Suzuki, A. *Synth. Commun.* **1981**, *11*, 513–519.
- (18) Litke, A. F.; Dai, C.; Fu, G. C. *J. Am. Chem. Soc.* **2000**, *122*, 4020–4028.
- (19) Stambuli, J. P.; Bühl, M.; Hartwig, J. F. *J. Am. Chem. Soc.* **2002**, *124*, 9346–9347.

rides²⁰ and even alkyl halides and related substrates.^{21–27} In many cases, it is clear that even minor changes in ligand can make the difference between a high-yielding catalyst and an inactive one.^{21,22,28} The extent of interest in new types of ligands for Suzuki coupling catalysts is exemplified by at least 10 references in 2004 alone on new phosphines,^{29–38} with focus on ones which are sterically demanding and/or hemilabile, favoring more rapid catalysis. In addition, other catalytic C–C, C–O, and C–N bond-forming reactions on C–X (X = halide or sulfonate) are facilitated by using sterically demanding phosphines.^{39–44}

The large phosphines used have included P(*t*-Bu)₃, which can be used to make the isolable, air-stable species Pd[P(*t*-Bu)₃]₂.^{45,46} There is considerable evidence that even this coordinatively unsaturated species loses a ligand, producing a catalytically active 12-electron monophosphine intermediate.^{18,19,47}

Hybrid ligands offer a way to stabilize low-coordinate species with a weakly coordinating ligand which can readily be removed from the metal, facilitating catalytic reactions. The most intensive study has been on hybrid P–O- and P–N-based ligands, which can show large and useful differences in binding affinity of the soft P and hard O or N donors for a given metal, which may itself be hard or soft.⁴⁸ For example, on related Ni(0) complexes, the hybrid ligand (*i*-Pr)₂PCH₂CH₂PNMe₂ afforded good yields of organic products, whereas the analogous chelating bis(phosphine) (*i*-Pr)₂PCH₂CH₂P(*i*-Pr)₂ either gave no or little product.^{49,50} These differences were ascribed to the

ability of the N donor in the hybrid complex to dissociate from the Ni(0) center during the catalytic cycle. In addition, the hybrid, hemilabile ligands in Rh complex **A** were found to



facilitate the carbonylation of methyl iodide in comparison with conventional monodentate trialkylphosphines in related systems.⁵¹ Effects of oxygen substituents on rate and selectivity of hydrogenation and hydroformylation have been noted.^{6,52} Among complexes with P–N-based hybrid ligands, those with pyrid-2-yl-modified phosphorus ligands were found to improve selectivity in hydroformylation of some olefins.^{53,54}

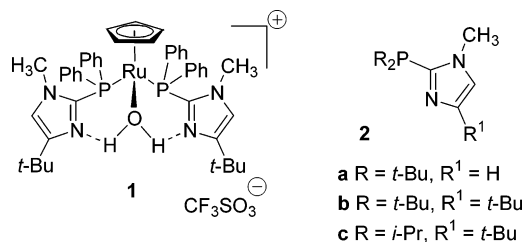
In this contribution we describe a new group of phosphine ligands which are sterically demanding because of two large alkyl groups on P and which are hybrid because the third substituent is an imidazol-2-yl unit. For comparison, in recent years, a great deal of attention has been drawn to 2-pyridylphosphines,⁵⁵ mainly as bridging ligands; however, despite synthesis of literally hundreds of their complexes there have been surprisingly few improved catalysts using such bifunctional ligands.^{56–59} By contrast, complexes of imidazolylphosphines have been much less-studied. Ligands with three imidazole groups have been used as tridentate (N)₃ ligands, bioinorganic models for three histidines in a protein.^{60–64} In these species the phosphorus is not bound to the metal and only serves as a connecting element. There have been a few reports of imidazolylphosphines as bridging ligands,^{65–73} bound through both

- (20) Littke, A. F.; Fu, G. C. *Angew. Chem., Int. Ed.* **2002**, *41*, 4176–4211.
- (21) Netherton, M. R.; Dai, C.; Neuschütz, K.; Fu, G. C. *J. Am. Chem. Soc.* **2001**, *123*, 10099–10100.
- (22) Kirchhoff, J. H.; Dai, C.; Fu, G. C. *Angew. Chem., Int. Ed. Engl.* **41**, 1945–1947.
- (23) Kirchhoff, J. H.; Netherton, M. R.; Hills, I. D.; Fu, G. C. *J. Am. Chem. Soc.* **2002**, *124*, 13662–13663.
- (24) Netherton, M. R.; Fu, G. C. *Angew. Chem., Int. Ed.* **2002**, *41*, 3910–3912.
- (25) Menzel, K.; Fu, G. C. *J. Am. Chem. Soc.* **2003**, *125*, 3718–3719.
- (26) Lee, J.-Y.; Fu, G. C. *J. Am. Chem. Soc.* **2003**, *125*, 5616–5617.
- (27) Zhou, J.; Fu, G. C. *J. Am. Chem. Soc.* **2003**, *125*, 12527–12530.
- (28) Hills, I. D.; Netherton, M. R.; Fu, G. C. *Angew. Chem., Int. Ed.* **2003**, *42*, 5749–5752.
- (29) DeVasher, R. B.; Moore, L. R.; Shaughnessy, K. H. *J. Org. Chem.* **2004**, *69*, 7919–7927.
- (30) Smith, R. C.; Woloszynek, R. A.; Chen, W.; Ren, T.; Protasiewicz, J. D. *Tetrahedron Lett.* **2004**, *45*, 8327–8330.
- (31) Baillie, C.; Zhang, L.; Xiao, J. *J. Org. Chem.* **2004**, *69*, 7779–7782.
- (32) Brenstrum, T.; Gerritsma, D. A.; Adjabeng, G. M.; Frampton, C. S.; Britten, J.; Robertson, A. J.; McNulty, J.; Capretta, A. *J. Org. Chem.* **2004**, *69*, 7635–7639.
- (33) Colacot, T. J.; Shea, H. A. *Org. Lett.* **2004**, *6*, 3731–3734.
- (34) Kwong, F. Y.; Lam, W. H.; Yeung, C. H.; Chan, K. S.; Chan, A. S. C. *Chem. Commun.* **2004**, 1922–1923.
- (35) Weng, Z.; Teo, S.; Koh, L. L.; Hor, T. S. A. *Organometallics* **2004**, *23*, 4342–4345.
- (36) Weissman, H.; Shimon, L. J. W.; Milstein, D. *Organometallics* **2004**, *23*, 3931–3940.
- (37) Wang, A.-E.; Zhong, J.; Xie, J.-H.; Li, K.; Zhou, Q.-L. *Adv. Synth. Catal.* **2004**, *346*, 595–598.
- (38) Harkal, S.; Rataboul, F.; Zapf, A.; Fuhrmann, C.; Riermeier, T.; Monses, A.; Beller, M. *Adv. Synth. Catal.* **2004**, *346*, 1742–1748.
- (39) Hartwig, J. F. *Acc. Chem. Res.* **1998**, *31*, 852–860.
- (40) Hartwig, J. F. *Angew. Chem., Int. Ed. Engl.* **1998**, *37*, 2046–2067.
- (41) Hartwig, J. F. In *Modern Amination Methods*; Ricci, A., Ed.; Wiley-VCH: Weinheim, Germany, 2000.
- (42) Hartwig, J. F. In *Handbook of Organopalladium Chemistry for Organic Synthesis*; Negishi, E., Ed.; Wiley: Hoboken, NJ, 2002; pp 1051–1096.
- (43) Wolfe, J. P.; Wagaw, S.; Marcoux, J.-F.; Buchwald, S. L. *Acc. Chem. Res.* **1998**, *31*, 805–818.
- (44) Yang, B. H.; Buchwald, S. L. *J. Organomet. Chem.* **1999**, *576*, 125–146.
- (45) Matsumoto, M.; Yoshioka, H.; Nakatsu, K.; Yoshida, T.; Otsuka, S. *J. Am. Chem. Soc.* **1974**, *96*, 3322–3324.
- (46) Otsuka, S.; Yoshida, T.; Matsumoto, M.; Nakatsu, K. *J. Am. Chem. Soc.* **1976**, *98*, 5850–5858.
- (47) Hartwig, J. F.; Paul, F. *J. Am. Chem. Soc.* **1995**, *117*, 5373–5374.
- (48) Pearson, R. G.; Scott, A. In *Survey of Progress in Chemistry*; Academic Press: New York, 1969; Chapter 1.
- (49) Müller, C.; Lachicotte, R. J.; Jones, W. D. *Organometallics* **2002**, *21*, 1975–1981.

- (50) Perthuisot, C.; Edelbach, B. L.; Zubris, D. L.; Simhai, N.; Iverson, C. N.; Müller, C.; Satoh, T.; Jones, W. D. *J. Mol. Catal. A: Chem.* **2002**, *189*, 157–168.
- (51) Lindner, E.; Andres, B. *Chem. Ber.* **1988**, *121*, 829–832.
- (52) Horner, L.; Simons, G. *Z. Naturforsch. B: Chem. Sci.* **1984**, *39*, 497–503.
- (53) Basoli, C.; Botteggi, C.; Cabras, M. A.; Chelucci, G.; Marchetti, M. *J. Organomet. Chem.* **1995**, *488*, C20–C22.
- (54) Kurtev, K.; Ribola, D.; Jones, R. A.; Cole-Hamilton, D. J.; Wilkinson, G. *J. Chem. Soc., Dalton Trans.* **1980**, 55–58.
- (55) Newkome, G. R. *Chem. Rev.* **1993**, *93*, 2067–2089.
- (56) Drent, E.; Arnoldy, P.; Budzelaar, P. H. M. *J. Organomet. Chem.* **1994**, *475*, 57–63.
- (57) Drent, E.; Arnoldy, P.; Budzelaar, P. H. M. *J. Organomet. Chem.* **1993**, *455*, 247–253.
- (58) Drent, E.; Van Broekhoven, J. A. M.; Doyle, M. J. *J. Organomet. Chem.* **1991**, *417*, 235–251.
- (59) 3- and 4-Pyridylphosphines have been used recently as bridging ligands to assemble polynuclear catalysts: Slagt, V. F.; Kamer, P. C. J.; Van Leeuwen, P. W. N. M.; Reek, J. N. H. *J. Am. Chem. Soc.* **2004**, *126*, 1526–1536. Slagt, V. F.; Reek, J. N. H.; Kamer, P. C. J.; Van Leeuwen, P. W. N. M. *Angew. Chem., Int. Ed.* **2001**, *40*, 4271–4274. Kleij, A. W.; Lutz, M.; Spek, A. L.; van Leeuwen, P. W. N. M.; Reek, J. N. H. *Chem. Commun. (Cambridge)* **2005**, 3661–3663.
- (60) Slebocka-Tilk, H.; Cocho, J. L.; Frackman, Z.; Brown, R. S. *J. Am. Chem. Soc.* **1984**, *106*, 2421–2431.
- (61) Brown, R. S.; Zamkane, M.; Cocho, J. L. *J. Am. Chem. Soc.* **1984**, *106*, 5222–5228.
- (62) Sorrell, T. N.; Allen, W. E.; White, P. S. *Inorg. Chem.* **1995**, *34*, 952–960.
- (63) Kimblin, C.; Bridgewater, B. M.; Churchill, D. G.; Parkin, G. *Dalton* **2000**, 2191–2194.
- (64) Kimblin, C.; Murphy, V. J.; Hascall, T.; Bridgewater, B. M.; Bonanno, J. B.; Parkin, G. *Inorg. Chem.* **2000**, *39*, 967–974.
- (65) Burini, A.; Pietroni, B. R.; Galassi, R.; Valle, G.; Calogero, S. *Inorg. Chim. Acta* **1995**, *229*, 299–305.
- (66) Burini, A.; Galassi, R.; Pietroni, B. R.; Rafaiani, G. *J. Organomet. Chem.* **1996**, *519*, 161–167.
- (67) Bachechi, F.; Burini, A.; Galassi, R.; Macchioni, A.; Pietroni, B. R.; Ziarelli, F.; Zuccaccia, C. *J. Organomet. Chem.* **2000**, *593–594*, 392–402.

P and N, but fewer of mononuclear complexes such as the ones described in this paper.^{71–77}

Our interest in imidazolylphosphines stems from our 2001 report⁷⁵ of a catalyst for anti-Markovnikov hydration of terminal alkynes to aldehydes which was more than 90 times faster than the best catalyst reported elsewhere in the literature. This species (**1**) contains two phosphines of general formula **2**, each bearing



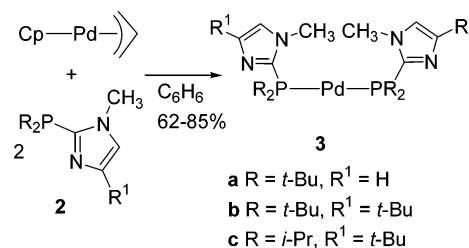
an imidazol-2-yl group capable of hydrogen bonding or proton transfer. In our further studies both published⁷⁸ and ongoing, we seek to clarify the effects on organometallic structure and catalysis of secondary interactions between basic or acidic phosphine substituents and other ligands such as water or amines. Thus, in this report we describe the preparation of several new bulky or chelating imidazolylphosphines, their complexation to both Pd(0) and Pd(II) centers, and the effects of the heterocycles on reactivity and binding to amines, which is shown to involve hydrogen bonding as a secondary interaction.

Results and Discussion

Synthesis and Structures of Two-Coordinate Complexes.

Hindered phosphines of type **2** were made by lithiating the appropriate 1-methylimidazole derivative with *n*-BuLi in THF,^{79,80} followed by quenching with the requisite chloro(dialkyl)-phosphine, as others have done using chloro(diphenyl)phosphine.⁶⁵ Our initial efforts to make Pd(0) species **3** used two moles of hindered phosphines **2** and Pd(dba)₂ (dba = dibenzylideneacetone). Monitoring these reactions by ¹H and ³¹P{¹H} NMR suggested that indeed zero-valent Pd complexes were formed cleanly, but efforts to remove the byproduct dba by recrystallization were never completely successful. Some previous literature efforts to make Pd–phosphine complexes Pd(dba)₂ have led to Pd–bis(phosphine) species but others have led to Pd–phosphine–dba complexes.^{81,82} Thus, the Pd(II)

Scheme 1. Preparation of Pd(0) Complexes **3**



precursor CpPd(allyl) was used as done by Otsuka et al.,^{45,46} forming volatile and very soluble hydrocarbon byproducts presumed to be isomers of allylcyclopentadiene. These byproducts could be completely and easily removed from crystalline, nonvolatile **3**, isolated in 62–85% yield (Scheme 1).

Elemental analyses for **3a**, **b**, **c** were consistent with ML₂ species. Spectroscopic data for **3a**, **b**, **c** (Tables 1 and 2) were consistent with formation of species with two equivalent phosphines mutually trans: the ³¹P{¹H} NMR spectra exhibited one sharp singlet in each case, and the ¹H and ¹³C{¹H} resonances for the atoms of the alkyl substituents on phosphorus and C-2 of the imidazol-2-yl groups appeared as virtual triplets. For example, the proton resonances for the *tert*-butyl groups in **3a** appeared at δ 1.55 ppm (vt, *N* = 13.8 Hz), and the carbon resonance for C-2 appeared at 144.6 ppm (vt, *N* = 37.7 Hz).⁸³

One key question unanswered by the spectroscopic data was whether the imidazole nitrogens were interacting with the metal. Intriguingly, for Pd(0) species **3a**, **b**, **c**, the protons of the *N*-methyl groups resonated as sharp singlets about 1 ppm downfield compared with the free ligands. Additional information about the bonding of the ligands required X-ray diffraction studies.

Crystals of **3a** were grown for analysis by X-ray diffraction. The data for refinement are given in Table 5 (Experimental Section), selected bond lengths and angles are shown in Table 3, and the ORTEP diagram of the structure is shown in Figure 1.

As shown in Figure 1, the Pd(0) complex **3a** adopted a nearly linear configuration (P–Pd–P angle, 174.0°), and when viewed down the P–P axis, the two imidazole rings are essentially gauche to each other, rather than anti. Interestingly, both of the imidazole *N*-methyl groups were pointed toward the Pd atom, consistent with agostic interactions. The distances between Pd atom and H atoms on the *N*-methyl group fell within the range of M–H distance for agostic interaction (1.85 to 2.4 Å). However, in general, a hydrogen involved in an agostic interaction shows some spectral data resembling those of a metal hydride, for example, in upfield ¹H NMR resonances^{84,85} or low-frequency C–H stretching absorptions in IR spectra (2300–2700 cm^{–1}).⁸⁶ Evidence against agostic interactions includes the 1.0 ppm-downfield ¹H NMR chemical shift of the *N*-methyl protons on complexation of the ligand, and normal C–H

- (68) Done, M. C.; Rüther, T.; Cavell, K. C.; Kilner, M.; Peacock, E. J.; Braussaud, N.; Skelton, B. W.; White, A. J. *Organomet. Chem.* **2000**, 607, 78–92.
 (69) Bachechi, F.; Burini, A.; Fontani, M.; Galassi, R.; Macchioni, A.; Pietroni, B. R.; Zanello, P.; Zuccaccia, C. *Inorg. Chim. Acta* **2001**, 323, 45–54.
 (70) Jalil, M. A.; Yamada, T.; Fujinami, S.; Honjo, T.; Nishikawa, H. *Polyhedron* **2001**, 20, 627–633.
 (71) Tejfel, C.; Bravi, R.; Ciriano, M. A.; Oro, L. A.; Bordonaba, M.; Graiff, C.; Tiripicchio, A.; Burini, A. *Organometallics* **2000**, 19, 3115–3119.
 (72) Tejfel, C.; Ciriano, M. A.; Bravi, R.; Oro, L. A.; Graiff, C.; Galassi, R.; Burini, A. *Inorg. Chim. Acta* **2003**, 347, 129–136.
 (73) Espino, G.; Jalon, F. A.; Maestro, M.; Manzano, B. R.; Perez-Manrique, M.; Bacigalupe, A. C. *Eur. J. Inorg. Chem.* **2004**, 2542–2552.
 (74) Moore, S. S.; Whitesides, G. M. *J. Org. Chem.* **1982**, 47, 1489–1493.
 (75) Grotjahn, D. B.; Incarvito, C. D.; Rheingold, A. L. *Angew. Chem., Int. Ed.* **2001**, 40, 3884–3887.
 (76) Caballero, A.; Jalon, F. A.; Manzano, B. R.; Espino, G.; Perez-Manrique, M.; Mucientes, A.; Poblete, F. J.; Maestro, M. *Organometallics* **2004**, 23, 5694–5706.
 (77) For a recent report on the use of *N*-aryl-2-phosphino(benz)imidazoles as ligands in Suzuki couplings and aryl aminations, see ref 38.
 (78) Grotjahn, D. B.; Lev, D. A. *J. Am. Chem. Soc.* **2004**, 126, 12232–12233.
 (79) Shirley, D. A.; Alley, P. W. *J. Am. Chem. Soc.* **1957**, 79, 4922–4927.
 (80) Curtis, N. J.; Brown, R. S. *J. Org. Chem.* **1980**, 45, 4038–4040.
 (81) Paul, F.; Patt, J.; Hartwig, J. F. *Organometallics* **1995**, 14, 3030–3039.

- (82) Herrmann, W. A.; Thiel, W. R.; Brossmer, C.; Oefele, K.; Priemeier, T.; Scherer, W. *J. Organomet. Chem.* **1993**, 461, 51–60.
 (83) The proton and carbon resonances for this complex were assigned using COSY, HMQC, and HMBC spectra, results summarized in Supporting Information.
 (84) Brookhart, M.; Green, M. L. H. *J. Organomet. Chem.* **1983**, 250, 395–408.
 (85) Brookhart, M.; Green, M. L. H.; Wonk, L.-L. *Prog. Inorg. Chem.* **1988**, 36, 1–124.
 (86) Elschenbroich, C.; Salzer, A. *Organometallics: A Concise Introduction*; 2nd ed.; VCH: Weinheim, 1992.

Table 1. ^1H and $^{31}\text{P}\{^1\text{H}\}$ NMR Data for Ligands and Pd Complexes^a

cmpd	solvent	¹ H						³¹ P{ ¹ H}
		Im-H5	H4 or R ¹ at C4	N-CH ₃	R ₂ P	other ligand(s) on Pd		
2a	CDCl ₃	6.96 (dd, 3, 1, 1H)	7.21 (br s, 1H)	3.81 (s, 3H)	1.18 (d, 7, 18H)	—	0.5	
2b	CDCl ₃	6.63 (d, 3, 1H)	1.27 (s, 9H)	3.75 (s, 3H)	1.21 (d, 7.2, 18H)	—	−0.4	
2c	CDCl ₃	6.63 (d, 2, 1H)	1.26 (s, 9H)	3.72 (d, 1, 3H)	0.96 (dd, <i>J</i> = 7, 12, 6H) 1.08 (dd, <i>J</i> = 7, 16, 6H) 2.32 (sept of d, <i>J</i> = 7, 2, 2H)	—	−19.3	
3a	C ₆ D ₆	6.31 (s, 2H)	7.30 (s, 2H)	4.31 (s, 6H)	1.55 (vt, <i>N</i> = 13.8, 36H)	—	32.4 (s)	
3b	C ₆ D ₆	6.37 (s, 2H)	1.43 (s, 18H)	4.34 (s, 6H)	1.56 (vt, <i>N</i> = 13.8, 36H)	—	32.1 (s)	
3c	C ₆ D ₆	6.34 (s, 2H)	1.45 (s, 18H)	4.12 (s, 6H)	1.22 (dvt, <i>J</i> = 7.5, <i>N</i> = 15.0, 12H) 1.29 (dvt, <i>J</i> = 6.0, <i>N</i> = 12.5, 12H) 2.59 (sept, 7.0, 4H)	—	16.2 (s)	
4c-PhI	C ₆ D ₆	6.36 (s, 2H)	1.39 (s, 18H)	3.80 (s, 6H)	1.08 (dvt, <i>J</i> = 7.6, <i>N</i> = 15.1, 12H) 1.39 (s, br, 12H) 2.66 (s, br, 4H)	6.62 (t, 7.1, 1H) 6.87 (t, 7.1, 2H) 7.16–7.18 (m, 2H)	13.7 (s)	
4c-MeOTf	C ₆ D ₆	6.39 (s, 2H)	1.39 (s, 18H)	3.60 (s, 6H)	1.14 (dvt, <i>J</i> = 7.2, <i>N</i> = 14.4, 12H) 1.23 (dvt, <i>J</i> = 8.8, <i>N</i> = 16.2, 12H) 3.03 (s, br, 4H)	0.22 (t, 6.2, 3H)	24.5 (s)	
4c-MeI	CD ₂ Cl ₂	6.78 (s, 2H)	1.27 (s, 18H)	3.86 (s, 6H)	1.15 (dvt, <i>J</i> = 7.2, <i>N</i> = 14.4, 12H) 1.30 (dvt, <i>J</i> = 7.2, <i>N</i> = 14.4, 12H) 3.39 (s, br, 4 H)	0.20 (t, 6.0, 3H)	21.4 (s)	
5a-PhBr	CDCl ₃	7.05 (s, 1H)	7.34 (s, 1H)	3.89 (s, 3H)	1.43 (d, 15.8, 18H)	6.79 (t, 7.2, 1H) 6.94 (t, 7.2, 2H) 7.37–7.42 (m, 2H)	43.5 (s)	
5a-PhI	CD ₂ Cl ₂	7.13 (s, 1H)	7.29 (s, 1H)	3.89 (s, 3H)	1.42 (d, 15.8, 18H)	6.80 (t, 7.6, 1H) 6.94 (t, 7.6, 2H) 7.25–7.41 (m, 2H)	36.9 (s)	
5b-PhI	CDCl ₃	6.73 (s, 1H)	1.37 (s, 9H)	3.84 (s, 3H)	1.45 (d, 15.6, 18H)	6.73 (t, 7.2, 1H) 6.91 (t, 7.2, 2H) 7.37–7.42 (m, 2H)	29.3 (s)	
[6a-Me]⁺[OTf][−]	CDCl ₃	7.12 (s,1H) 7.29 (s, br, 2H) ^b	5.18 (s, 1H)	3.97 (s, 6H)	1.29–1.73 (m, 36H)	0.95 (t, 5.2, 3H)	32.1 (s)	
	CDCl ₃ ^c	7.12 (s, 1H) 7.28 (s, 1H)	5.18 (s, 1H) 7.30 (s, 1H)	3.95 (s, 3H) 3.99 (s, 3H)	1.29 (vt, <i>N</i> = 14.4, 9H) 1.47 (vt, <i>N</i> = 16.0, 18H) 1.67 (s, br, 9H)	0.95 (t, 5.2, 3H)	32.1 (s)	
7c-CH₂Cl₂	CD ₂ Cl ₂	7.56 (s, 1H)	1.41 (s, 9H)	3.97 (s, 3H)	1.25 (dd, <i>J</i> = 7.5, 18.0, 6H) 1.56 (dd, <i>J</i> = 7.0, 19.0, 6H) 2.87 (sept of d, <i>J</i> = 7.0, 11.0, 2H)	4.56 (d, 2.0, 2H, PdCH ₂ N)	65.3 (s)	
[8b-Ph]⁺[OTf][−]	CD ₂ Cl ₂	7.04 (s, 1H)	1.31 (s, 9H)	3.91 (s, 3H)	1.41 (d, 16.2, 18H)	7.03 (m, 1H) 7.09 (m, 2H) 7.41 (m, 2H) 1.27 (d, 6.2, 6H, amine CH ₃) 2.65–2.77 (m, 1H)	39.8 (s)	
[8a-Ph]⁺[B(ArF[′])₄][−]	CD ₂ Cl ₂	7.17 (s, 1H)	7.22 (s, 1H)	3.92 (s, 3H)	1.41 (d, 16.4, 18H)	1.35 (d, 7.8, 6H) 2.57 (br s, 2H) 3.28 (sept, 6.6, 1H) 7.00 (t, 7.0, 1H) 7.08 (t, 7.2, 2H) 7.29–7.37 (m, 2H)	45.4 (s)	
[9b-Ph]⁺[OTf][−]	CD ₂ Cl ₂	7.10 (s, 1H)	1.34 (s, 9H)	3.92 (s, 3H)	1.39 (d, 16.5, 18H)	2.74 (dt, 11.0, 12.0, 2H) 3.04 (d, 13.5, 2H) 3.34 (t, br, 12.0, 1H) 3.50 (t, 11.5, 2H) 3.78 (d, 13.0, 2H) 7.04 (t, 7.5, 1H) 7.10 (t, 8.0, 2H) 7.39–7.42 (m, 2H)	42.3 (s)	
[10c-Me]⁺[OTf][−]	CD ₂ Cl ₂	6.69 (s, 2H)	1.12 (s, 18H)	4.00 (s, 6H)	1.18–1.38 (m, 24H) 2.80–3.05 (m, 4H)	0.51 (t, 6.2, 3H) 2.95–3.10 (m, 2H) 3.44 (br s, 2H) 6.29 (sl br d, 6, 2H) 7.10–7.22 (m, 3H)	30.3 (s)	
	CDCl ₃	6.93 (s, 2H)	1.11 (s, 18H)	4.04 (s, 6H)	1.25–1.32 (m, 24H) 2.92 (septet, 6.5, 4H)	0.47 (t, 6.0, 3H) 3.03 (t,7.0, 2H) 3.30 (br s, 2H) 6.33 (sl br d, 7.0, 2H) 7.11–7.20 (m, 3H)	28.8 (s)	
[10c-Me]⁺[B(ArF[′])₄][−]	CDCl ₃	6.87 (s, 2H)	1.11 (s, 18H)	3.94 (s, 6H)	1.25–1.32 (m, 24H) 2.89 (sept, 6.5, 4H)	0.50 (t, 6.0, 3H) 3.00 (t, 7.5, 2H) 3.41 (s, br, 2H) 6.20 (d,7.5, 2H) 7.11 (t, 7.5, 2H) 7.18 (t, 7.5, 1H)	30.5 (s)	

^a Measured at 30 °C unless otherwise specified. Chemical shifts in ppm, δ scale. Unless otherwise stated, value after multiplicity is *J* in Hz. br = broad.^b Peak for H-4 and H-5 overlapping at this temperature but separated at −50 °C. ^c Measured at −50 °C.

Table 2. $^{13}\text{C}\{^1\text{H}\}$ NMR Data for Ligands and Pd Complexes^a

compd	C-2	C-4	C-5	R ¹ at C-4	CH ₃ at N-1	R ₂ P	other ligand(s) on Pd
2a	158.4 (s)	129.8 (s)	122.4 (s)	—	33.3 (d, 14) ^b	30.1 [d, 14, C(CH ₃) ₃] 34.6 (d, 18) ^b	—
2b	153.2 (d, 1)	143.6 (d, 10.4)	115.7 (d, 1.4)	30.4 [s, C(CH ₃) ₃] 32.1 [s, C(CH ₃) ₃]	34.1 (d, 16.8)	30.2 [d, 14.1, C(CH ₃) ₃] 33.5 [d, 14.1, C(CH ₃) ₃]	—
2c	153.6 (d, 1)	144.9 (d, 9)	116.2 (s)	30.4 [s, C(CH ₃) ₃] 32.0 [s, C(CH ₃) ₃]	33.7 (d, 15)	19.4 (d, 8, CHMeMe) 20.1 (d, 18, CHMeMe) 24.39 (s, one CHMe ₂) 24.44 (s, other CHMe ₂)	—
3a	144.6 (vt, <i>N</i> = 37.7)	130.0 (vt, <i>N</i> = 6.2)	123.6 (s)	—	37.2 (vt, <i>N</i> = 13.8)	31.5 (vt, <i>N</i> = 11.7) 36.8 (vt, <i>N</i> = 14.7)	—
3b	143.3 (vt, <i>N</i> = 36.3)	152.8 (vt, <i>N</i> = 5.8)	117.4 (s)	30.9 (s) 32.5 (s)	37.2 (vt, <i>N</i> = 13.8)	31.6 (vt, <i>N</i> = 11.8) 36.5 (vt, <i>N</i> = 14.2)	—
3c	142.8 (vt, <i>N</i> = 41.0)	153.4 (s)	117.9 (s)	30.9 (s) 32.6 (s)	36.0 (broad)	21.2 (s, broad) 20.2 (s, sharp) 27.4 (vt, <i>N</i> = 21.0)	—
4c-PhI	140.1 (vt, <i>N</i> = 67.5)	153.2 (vt, <i>N</i> = 8.4)	118.2 (s)	30.8 (s) 32.4 (s)	37.0 (s)	20.5 (s, sharp) 21.0 (s, broad) 27.7 (vt, <i>N</i> = 26.0)	123.8 (s, C-4) 127.5 (s, C-3) 138.5 (t, 16.3, C-2) 153.2 (t, 4.4, C-1) —6.2 (s)
4c-MeOTf	135.7 (vt, <i>N</i> = 64.9)	154.4 (vt, <i>N</i> = 8.3)	119.5 (s)	30.6 (s) 32.5 (s)	35.4 (s)	19.0 (s) 20.0 (s) 24.9 (vt, <i>N</i> = 24.9)	—
5a-PhI	147.8 (d, 27.9)	129.9 (d, 12.2)	126.2 (s)	—	36.9 (s)	30.3 (d, 6.0) 37.2 (d, 6.8)	122.7 (s, C-4) 126.8 (d, 2.3, C-3) 138.3 (d, 8.9, C-1) 139.1 (d, 4.7, C-2)
5b-PhI	146.6 (d, 30.4)	154.2 (d, 11.6)	119.6 (s)	30.5 (s) 32.0 (s)	36.7 (s)	30.3 (d, 5.8) 37.0 (d, 7.8)	122.4 (s, C-4) 126.5 (d, 2.0, C-3) 134.1 (d, 10.6, C-1) 139.0 (d, 4.5, C-2) —17.2 (s)
[6a-Me]⁺[OTf]^{−c}	139.5 (vt, <i>N</i> = 56.5) 145.8 (vt, <i>N</i> = 28.8)	127.6 (vt, <i>N</i> = 13.3) 130.3 (vt, <i>N</i> = 8.2)	124.8 (s) 127.3 (s)	—	36.6 (s) 37.2 (s)	30.2 (s) 30.4 (s) 36.3 (vt, <i>N</i> = 9.0) 36.7 (vt, <i>N</i> = 9.5) 38.4 (vt, <i>N</i> = 16.8) 38.6 (vt, <i>N</i> = 18.0)	—
7c-CH₂Cl₂	147.5 (d, 27.7)	146.2 (d, 8.6)	129.4 (s)	29.1 (s) 32.6 (s)	38.3 (s)	19.6 (d, 5.0) 20.2 (s) 27.5 (d, 24.4)	45.1 (d, 5.4, PdCH ₂ N)
[8b-Ph]⁺[OTf][−]	145.6 (d, 35.2)	153.5 (d, 10.3)	141.4 (s)	30.4 (s) 31.6 (s)	37.4 (s)	30.3 (d, 6.3) 37.5 (s)	25.7 (s, amine CH ₃) 46.5 (s, amine CHN) 121.7 (s, Ph-C4) 124.9 (s, Ph-C3) 128.8 (d, 2.1, Ph-C-2) 136.7 (d, 3.9, Ph-C-1)
[9b-Ph]⁺[OTf][−]	145.5 (d, 36.7)	153.0 (d, 10.0)	143.3 (s)	30.3 (s) 31.5 (s)	37.5 (s)	30.3 (d, 4.8) 37.6 (s)	49.3 (s, amine C-3) 68.2 (s, amine C-2) 122.1 (s, Ph-C4) 125.2 (s, Ph-C3) 128.6 (d, 2.0, Ph-C-2) 136.6 (d, 3.9, Ph-C-1) —10.4 (s, Pd-CH ₃)
[10c-Me]⁺[OTf][−]	134.2 (vt, <i>N</i> = 56.6)	154.3 (vt, <i>N</i> = 11.3)	121.3 (s)	29.8 (s) 31.7 (s)	35.8 (s)	19.2 (s) 23.9 (vt, <i>N</i> = 24.6)	49.1 (s, CH ₂) 127.7 (s, meta) 128.7 (s, para) 129.5 (s, ortho) 139.8 (s, ipso) —10.1 (s, Pd-CH ₃)
[10c-Me]⁺[B(ArF')₄]^{−d}	134.3 (vt, <i>N</i> = 56.3)	154.7 (vt, <i>N</i> = 10.8)	121.3 (s)	29.7 (s) 31.8 (s)	35.3 (s)	19.1 (s) 23.9 (vt, <i>N</i> = 24.6)	48.5 (s, CH ₂) 126.8 (s, meta) 128.3 (s, para) 129.0 (s, ortho) 138.8 (s, ipso)

^a Measured at 30 °C in same solvents as listed in Table 1, CD₂Cl₂ in the case of [10c-Me]⁺[OTf][−]. Chemical shifts in ppm, δ scale. Unless otherwise stated, value after multiplicity is *J* in Hz. br = broad. ^b Assignment of 33.3 and 34.6 ppm peaks not completely certain. ^c Measured at 0 °C. ^d Resonances for the anion: 148.2 (d of narrow m, *J* \approx 242, ortho C — furthest downfield), 138.2 (d of narrow m, *J* \approx 240, para C — about half the intensity of the signal at 136.2), 136.2 (d of narrow m, *J* \approx 240, meta C), 124.0 (very broad, ipso C).

stretching absorptions, between 2860 and 2960 cm^{−1}. Thus, although Figure 1 shows that the solid-state orientation of the methyl groups is consistent with agostic interaction with a 14-electron metal center, all the spectroscopic evidence lead us to the conclusion that there are no agostic interactions between Pd and H atoms of the *N*-methyl groups. Rather, the orientations seen for the imidazole rings may be a way for the system to

avoid steric interactions between the two bulky *tert*-butyl groups on the phosphorus atom and the *N*-methyl group on the imidazole. A similar orientation was seen by Otsuka et al. in their crystal structure of (*t*-Bu₂PPh)₂Pd,⁴⁶ and Milstein and co-workers recently reported a two-coordinate Pd(0) complex in which the hard ether oxygens are positioned to interact with the soft Pd(0) center but do not.³⁶ Clearly, a combination of

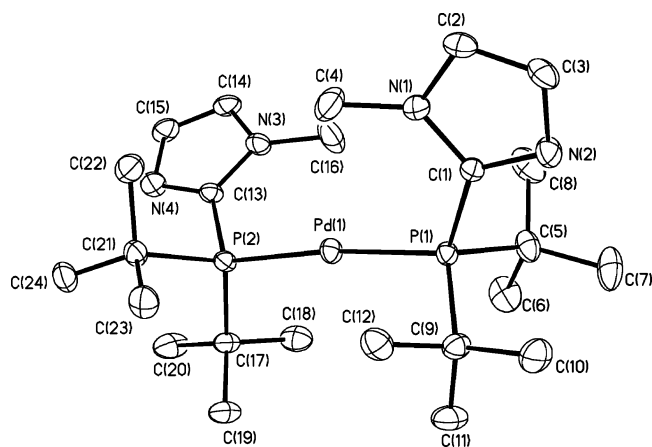
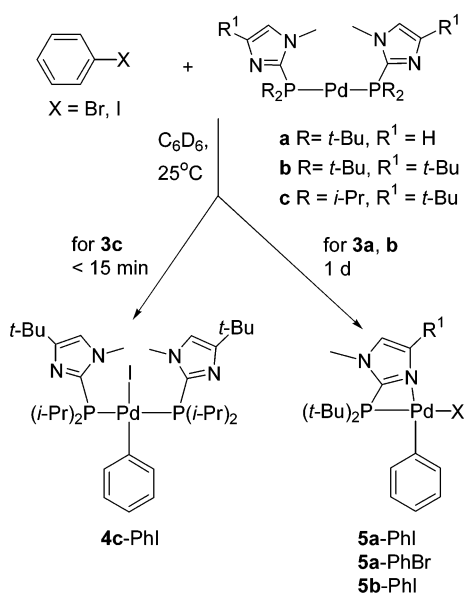


Figure 1. Molecular structure of **3a**. Ellipsoids are shown at 30% probability.

Scheme 2. Reactivity with Aryl Halides as a Function of Phosphine



structural and spectroscopic data are needed to establish whether a potentially coordinating ligand is truly hemilabile.

Reactivities of Pd(0) Complexes with Aryl Halides. In the coupling reaction between aryl halides and amines, oxidative addition of aryl halides is usually involved in the early stage of the catalytic cycle, generally following the dissociation of one ligand from the catalyst.^{18,19,47}

The oxidative addition products are likely intermediates in metal-catalyzed cross-coupling reactions. The low-coordinate, electron-rich Pd(0) complexes prepared above were expected to readily undergo oxidative addition with aryl halides.

Significantly, for reactions of Pd(0) complexes **3a, b, c** with aryl halides, reaction rates and product structures could be controlled by changing the X group on the aryl halide and the alkyl substituents on phosphorus (Scheme 2).

When the less crowded Pd(0) complex **3c** was treated with iodobenzene at room temperature, oxidative addition was complete within a remarkably short time, 15 min. The product, **4c-PhI** was soluble in benzene and was isolated by recrystallization in 71% yield. The molecular formula of the product was confirmed by elemental analysis, and the trans orientation

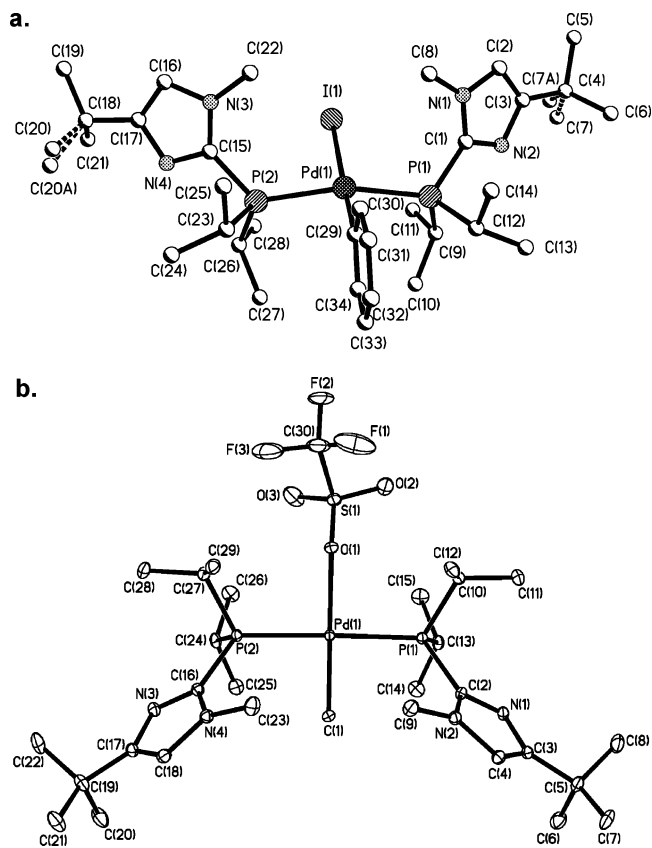
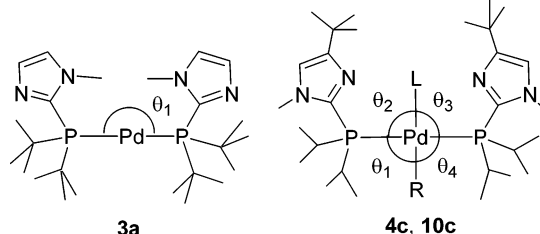


Figure 2. X-ray crystal structures of (a) **4c-PhI** and (b) **4c-MeOTf**. Ellipsoids are shown at 30% probability. In Figure 2a, carbons C7 and C20 were disordered over two positions in occupational multiplicity of 0.7 to 0.3, and were treated as anisotropic.

of the two equivalent phosphines was determined by a $^{31}\text{P}\{^1\text{H}\}$ singlet and the appearance of certain proton and carbon resonances as virtual triplets. For example, the proton resonances for methyl group on isopropyl substituent appeared at 1.08 ppm as doublet of virtual triplet, and the carbon resonance for C-2 of the imidazol-2-yl group appeared at 140.1 ppm (vt, $N = 67.5$ Hz). Moreover, the $^{31}\text{P}\{^1\text{H}\}$ NMR spectrum of **4c-PhI** showed a singlet, consistent with trans geometry. In confirmation, the molecular structure as confirmed by X-ray diffraction is shown in Figure 2a.

As expected, complex **4c-PhI** features a square-planar Pd center (the sum of the four L–Pd–L angles is 362° , Table 3), on which both of the phosphine ligands are located trans to each other, whereas the aryl and halide ligands occupied the other two coordination sites. Distortions in this symmetrical but crowded complex include a P–Pd–P angle of $163.71(3)^\circ$, which may be ascribed to interactions between isopropyl substituents on phosphines and the ring of the phenyl ligand (Figure 2a).

The reactions of aryl halides with Pd(0) complexes **3a, 3b** with more hindered phosphine ligands are different from that with **3c**. The rate of the reactions was quite a bit slower, requiring a period of 24 h. Iodobenzene reacted somewhat faster than bromobenzene and gave a better yield, 94–97% vs 72%. Most significantly, the structures of products from **3a** and **3b** were different than that of the product obtained from **3c**, and reactions followed different stoichiometry. The reactions of **3a** with either PhBr or PhI or of **3b** with PhI in C_6D_6 were monitored by NMR.

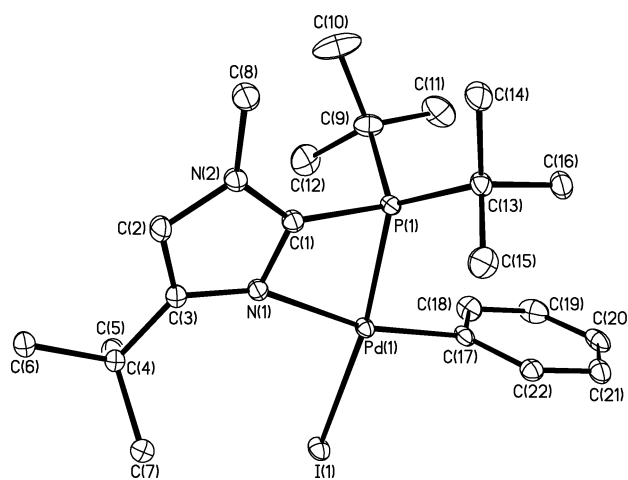
Table 3. Selected Bond Lengths (Å) and Bond Angles (deg) for Complexes **3a**, **4c**, and **10c**


	3a	4c-PhI	4c-MeOTf	[10c-Me][OTf][−]	[10c-Me][B(Ar^f)₄][−]
R	—	Ph	Me	Me	Me
L	—	I	OTf	NH ₂ CH ₂ Ph	NH ₂ CH ₂ Ph
Pd—P(1)	2.2836(4)	2.3430(8)	2.3328(5)	2.3448(7)	2.3387(8)
Pd—P(2)	2.2886(4)	2.3405(8)	2.3356(5)	2.3284(7)	2.3287(8)
Pd—L	—	2.6904(3)	2.2161(13)	2.148(2)	2.137(2)
Pd—R	—	2.021(3)	2.0436(19)	2.059(3)	2.077(3)
θ ₁	173.964(14)	93.00(2)	91.27(4)	94.49(6)	93.59(8)
θ ₂	—	88.88(8)	88.78(8)	86.86(9)	87.29(9)
θ ₃	—	88.71(8)	89.02(8)	86.81(9)	88.08(9)
θ ₄	—	91.98(2)	91.48(4)	93.11(6)	92.34(8)
N(Im)—N(amine)	—	—	—	2.883(5), 2.943(5)	2.885(4), 2.920(4)

Surprisingly, as the reaction proceeded, signals for the free phosphine appeared and grew until all the signals for complex **3a** or **3b** had disappeared. At the same time, yellow crystals precipitated out of the solution. The proton NMR spectra of a solution from the crystals in either CD₂Cl₂ or CDCl₃ revealed resonances for a phenyl ligand in the range 6.7–7.5 ppm. The singlet for the three *N*-methyl protons on the oxidative addition products shifted 0.4 ppm upfield compared to that of Pd(0) complexes. Significantly, the signals for the imidazole ring and the *tert*-butyl groups of the phosphine (in the case of reaction of **3a** with PhI, singlets at 7.13 and 7.29 ppm and doublet at 1.42 ppm) integrated for only 1, 1, and 18 protons, respectively, indicating that there was only one phosphine ligand in each complex; hence, the empirical formula would be (phosphine)-PdPhI. This composition was verified by elemental analysis in each case. However, we needed X-ray diffraction data to assign the hapticity of the imidazolylphosphine, the stereochemistry about the metal, and even the nuclearity of the complex.

Many previous arylpalladium halide complexes with a single hindered ligand, such as P(*o*-tol)₃, have been dimeric.^{81,87} Since the bridging halide palladium dimer has the same ratio of ligands as that of monomeric one, it is not possible to tell one from the other only based on NMR spectroscopic data. However the X-ray diffraction data of **5a-PhBr**, **5a-PhI**, and **5b-PhI** showed that the complexes are indeed monomeric. The structure of complex **5b-PhI** is shown in Figure 3, and selected bond lengths and angles are shown in Table 4, along with data for structures of **5a-PhBr** and **5a-PhI**. The structures of the latter are shown in Supporting Information.

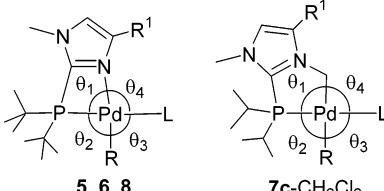
Figure 3 shows that **5b-PhI** has a distorted square-planar geometry, with the P and N atoms on the chelating phosphine ligand occupying two adjacent coordination sites while the phenyl ligand and halide ligand fill the other two, with phenyl trans to the N atom and halide trans to the P atom. The sum of the four intraligand angles is equal to 360.0° within experimental uncertainty, but the four-membered chelate ring has a narrow P—Pd—N angle [69.01(5)°], creating a large adjacent N—Pd—I angle [106.10(5)°].

**Figure 3.** Molecular structure of **5b-PhI**. Ellipsoids are shown at 30% probability.

Steric interactions between ligands become especially apparent (Table 4) in comparing the structure of **5a-PhI** which lacks the imidazole *tert*-butyl substituent (R¹) with that of **5b-PhI**, just discussed. Looking at Table 4, in going from **5a-PhI** to **5b-PhI** one sees essentially no change in bond lengths between Pd and the four ligands, with the important exception of the Pd—N(Im) distance, which is about 0.1 Å longer in the *tert*-butyl-substituted case. Similarly, ligand substitution has the largest effect on θ₄, the N(Im)—Pd—I angle, increasing it by 7.6° on going from **5a-PhI** to **5b-PhI**. This movement of the iodide ligand away from the coordinated heterocycle is compensated by the closing of intraligand angles θ₃ and θ₂ by 3.1 and 3.6°, respectively, with the remaining chelate bite angle hardly changing at all.

Not long after we isolated and resolved the structure of these monomeric complexes, Hartwig's group published a structure of a monomeric, three-coordinate T-shaped species (phosphine)-PdPhX with a hindered phosphine.¹⁹ As in our structures, the phosphine and halide ligands are trans to each other. Their structure features the phenyl group located trans to the open coordination site of the metal, whereas ours has the imidazole nitrogen in this position. The observed geometry of the T-shaped

(87) Widenhoefer, R. A.; Zhong, H. A.; Buchwald, S. L. *Organometallics* **1996**, *15*, 2745–2754.

Table 4. Selected Bond Lengths (Å) and Bond Angles (deg) for Chelate Complexes 5–8


	5a-PhBr	5a-PhI	5b-PhI	[6a-Me] ⁺ [OTf] [−]	7c-CH ₂ Cl ₂	[8b-Ph] ⁺ [OTf] [−]
R ¹	H	H	<i>t</i> -Bu	H	<i>t</i> -Bu	<i>t</i> -Bu
R	Ph	Ph	Ph	Me	Cl	Ph
L	Br	I	I	2a	Cl	NH ₂ CH(CH ₃) ₂
Pd–P(1)	2.2748(6)	2.2936(6)	2.2890(6)	2.3496(5)	2.1878(4)	2.2639(6)
Pd–L	2.4729(3)	2.6245(3)	2.6368(2)	2.3337(5)	2.3769(4)	2.129(2)
Pd–N(Im)	2.170(2)	2.1639(18)	2.2626(17)	2.1735(16)	2.0236(17) ^a	2.198(2)
Pd–R	1.988(2)	1.997(2)	1.995(2)	2.051(2)	2.4124(4)	1.979(2)
θ ₁	69.98(6)	69.76(5)	69.01(5)	68.96(5)	86.63(5)	70.14(5)
θ ₂	100.02(7)	100.18(7)	96.60(6)	97.71(6)	91.203(15)	99.01(6)
θ ₃	90.47(7)	91.55(7)	88.42(6)	94.13(6)	96.312(15)	86.43(10)
θ ₄	99.64(5)	98.50(5)	106.10(5)	99.07(5)	86.02(5)	104.78(9)

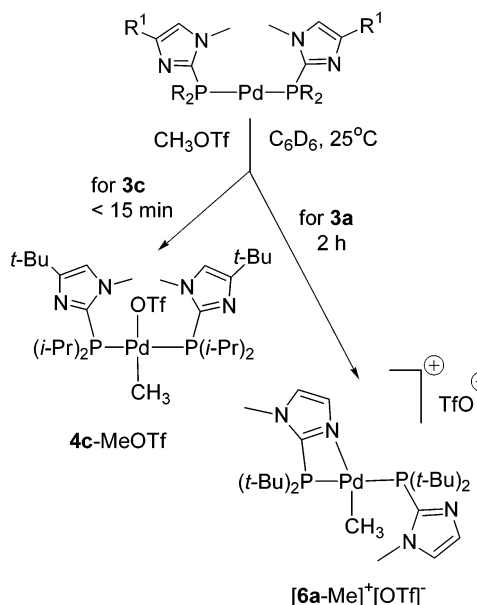
^a Length of bond between Pd and attached CH₂ carbon.

system allows the ligand with the greatest steric demand to bind in the least hindered position and the covalent ligand with the largest trans effect to bind trans to the open site. A similar reaction course (loss of one bulky ligand) and geometrical preference (ligands with highest trans effect i.e. P and aryl C, cis to each other) was seen recently by Milstein et al.³⁶

Comparing reactivities of **3a–3c** briefly at this point, we believe that changing steric demands of phosphine substituents (isopropyl in **3c** vs *tert*-butyl in **3a** or **3b**) determine not only the rate of oxidative addition (a phenomenon well-documented for other complexes elsewhere⁸⁸) but also the structure of the resulting oxidative addition products, a bis(phosphine) complex of type of **4c-PhI** or a monophosphine species such as **5a-** or **5b-PhX** with chelated phosphine. In addition, more subtle changes accompany heterocycle substitution. The ability of large substituents on phosphorus (e.g., R = *tert*-butyl in R₂PR') to promote interactions such as cyclometalation between atoms on R' and a metal coordinated to R₂PR' has been seen before, notably by Shaw and co-workers.⁸⁹ The work here shows that the same effects come to play in hemilabile systems.

Reactivities of Pd(0) Complexes with Methyl Triflate.

Similar to the reaction of **3c** with iodobenzene, reaction between **3c** and methyl triflate was fast and clean at room temperature (Scheme 3). The product **4c-MeOTf** is symmetrical, with the two phosphine ligands trans to each other and the remaining methyl and triflate ligands trans to each other. In the ¹H NMR spectrum, the resonances for methyl groups on each isopropyl substituent appeared at 1.14 and 1.23 ppm (each a doublet of virtual triplet), and the resonance for methyl protons on Pd–Me appeared at 0.22 ppm as a triplet (*J*_{P–H} = 6.2 Hz). The product was fairly soluble in benzene, suggesting a neutral species rather than an ionic one, a proposal confirmed by observation in the infrared spectrum of an S–O stretch absorption band at 1316 cm^{−1} for a bound triflate rather than free triflate ion.⁹⁰ Elemental analysis and ultimately X-ray

Scheme 3. Reactivity with Methyl Triflate and Product Structure as a Function of Phosphine

diffraction data were consistent with the structure (Figure 2b). The average Pd–P bond lengths in **4c-MeOTf** are 0.007 Å shorter in this complex than in **4c-PhI**, perhaps a reflection of the smaller sizes of the two anionic ligands. Consistent with this, in **4c-MeOTf**, the P–Pd–P angle is 173.353(18)°, whereas in **4c-PhI** it is 163.71(3)°, suggesting greater distortion in the latter complex.

The reaction between **3a** with methyl triflate in benzene required 2 h at room temperature, several times longer than the reaction with **3c**, consistent with the larger size of the ligands. Elemental analysis of the product was consistent with an oxidative addition product in which the two phosphines were retained, in distinct contrast to results from oxidative addition of haloarenes to **3a**, in which one phosphine was lost. To a first approximation, the proton and phosphorus NMR data for the product from **3a** suggested a structure similar to **4c-MeOTf**, but the product resulting from **3a** was much less soluble in benzene than the corresponding one from **3c**, and also the

(88) For older examples, see: Tolman, C. A. *Chem. Rev.* **1977**, 77, 313–348, and for more recent examples, see: Mann, G.; Shelby, Q.; Roy, A. H.; Hartwig, J. F. *Organometallics* **2003**, 22, 2775–2789 and Caporali, M.; Müller, C.; Staal, B. B. P.; Tooke, D. M.; Spek, A. L.; van Leeuwen, P. W. N. M. *Chem. Commun. (Cambridge)* **2005**, 3478–3480.

(89) Shaw, B. L. *J. Organomet. Chem.* **1980**, 200, 307–318.

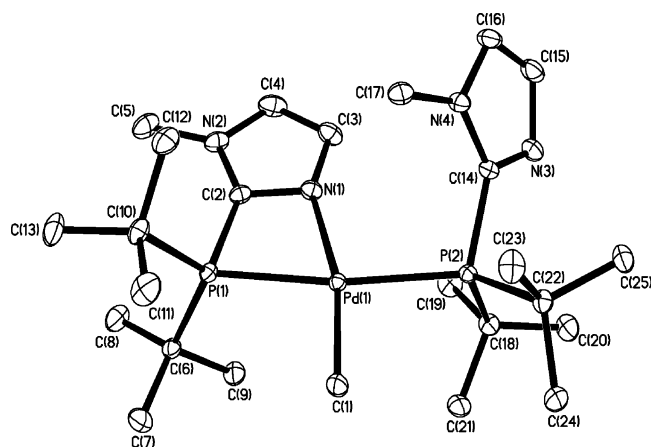


Figure 4. Molecular structure of $[6a-Me]^+[OTf]^-$. Only the cation is shown. Ellipsoids are shown at 30% probability.

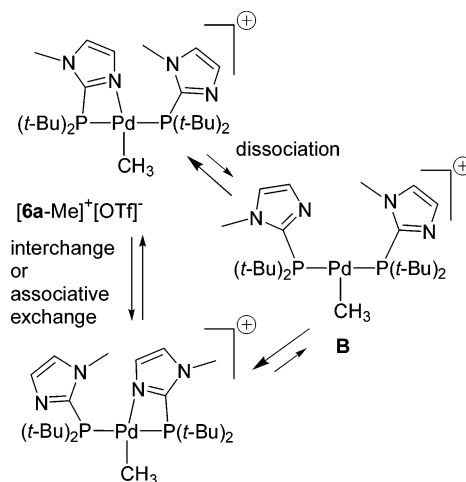
appearance of a strong IR absorption at 1271 cm^{-1} suggested an ionic triflate rather than a bound one.⁹⁰

At $30\text{ }^\circ\text{C}$, in CDCl_3 , the ^1H NMR spectrum (Table 1) showed a sharp triplet at 0.95 ppm (3H) and a sharp singlet at 3.97 ppm (6H) which were assigned to the methyl ligand on Pd and the imidazole *N*-methyl protons, respectively. One singlet at $\delta\ 32.1\text{ ppm}$ was found in the $^{31}\text{P}\{^1\text{H}\}$ NMR spectrum. On the basis of these NMR data, we would expect that the structure of the product is similar to that of **4c-MeOTf**, which is symmetrical. However, for the *tert*-butyl substituents on the phosphorus atoms were seen three broad peaks in the range $\delta\ 1.29\text{--}1.73\text{ ppm}$. The unusual appearance of these proton resonances, and in comparison with **4c-MeOTf**, the different solubility and the IR absorption led us to question this conclusion. Therefore, we grew crystals for X-ray analysis.

The X-ray data (Figure 4 and Table 4) showed that the product is the ionic species $[6a-Me]^+[OTf]^-$, indeed quite different from **4c-MeOTf**, explaining the different solubility and IR absorption spectra. The four angles around Pd center are added up to 359.9° indicating a square-planar geometry. The two phosphine ligands are located trans to each other, with one phosphine ligand chelating to the Pd center with an imidazole N atom and Pd–methyl ligand trans to the coordinated N atom. The angle N–Pd–P(1) is small (68.96°) because of the four-membered chelate ring. The triflate was found as a free ion rather than coordinating to the Pd as it does in **4c-MeOTf**, in accord with solution-phase IR data for both complexes. The Pd–P bond lengths are significantly longer (about 0.05 \AA) than those of **3a**, consistent with increased steric demand about the metal center and reduced back-bonding to the phosphines. In addition, the Pd–P bond lengths are longer (about 0.05 \AA) than in **5a-PhX** and **5b-PhI**, perhaps because of the higher trans influence of the second phosphine in $[6a-Me]^+[OTf]^-$.

According to the solid-state structure, the two phosphine ligands are inequivalent so that two sets of ligand resonances would be expected in ^1H NMR spectra, and two different phosphorus signals would be expected in $^{31}\text{P}\{^1\text{H}\}$ NMR spectra. Our NMR data collected at $30\text{ }^\circ\text{C}$ did not meet these expectations: in particular, resonances for imidazole aromatic hydrogens appeared broad, and more intriguingly, one of these resonances had an unusually high-field chemical shift of $\delta\ 5.18$

Scheme 4. Fluxionality in $[6a-Me]^+[OTf]^-$



ppm, suggesting an unusual environment for this unique proton. All these unexpected spectroscopic data raised these questions: Is the structure of the complex in solution the same as that of complex in solid state? Is there an equilibrium of two or more species in the solution? To which phosphine (chelated or unchelated) does the aromatic proton with high-field chemical shift belong?

To answer these questions, variable-temperature ^1H , $^{31}\text{P}\{^1\text{H}\}$, and $^{13}\text{C}\{^1\text{H}\}$ NMR spectra as well as NOE, DEPT, COSY, HMQC, and HMBC data were obtained. While the sample temperature was lowered, the broad signals for the *tert*-butyl groups in the ^1H NMR sharpened. At $-50\text{ }^\circ\text{C}$, all signals were sharp, and the presence of the two different phosphine ligands was suggested by two singlets for *N*-methyl protons and four singlets for imidazolyl protons, consistent with the solid-state structure. Rather remarkably, at $-50\text{ }^\circ\text{C}$ four virtual triplets for *tert*-butyl substituents were seen, consistent with each large alkyl group being in a unique environment both in the solid state and in solution. Our interpretation of these data is that at lower temperature the rotation of each ligand about the Pd–P axis is slowed to the point where four individual virtual triplets could be seen. On the other hand, when the temperature was increased, the resonances of aromatic protons on imidazole and *tert*-butyl substituents became broader and started to coalesce, while the resonance for the methyl–Pd ligand protons always stayed sharp. However, over the temperature range -50 to $+55\text{ }^\circ\text{C}$, only one singlet was detected in the $^{31}\text{P}\{^1\text{H}\}$ NMR spectrum.

The interesting dynamic behavior of $[6a-Me]^+[OTf]^-$ in solution (Scheme 4) can be explained by invoking a windshield-wiper exchange of the chelating and nonchelating ligands, either in a concerted interchange process or through a three-coordinate T-shaped intermediate **B**. By simulating the appearance of that portion of the spectrum for the four imidazole aromatic hydrogens, we determined for the site exchange of chelating and nonchelating imidazoles the following parameters: $E_a = 6 \pm 2\text{ kcal mol}^{-1}$ and $\Delta S^\ddagger = -6 \pm 4\text{ cal mol}^{-1}\text{ K}^{-1}$.⁹¹ We are aware of only a single recent report on such a process in imidazolylphosphine complexes, however, without data on the activation parameters.⁷³ There are a few examples in pyrid-2-ylphosphine chemistry of complexes with one chelating and one

(90) Stang, P. J.; Huang, Y. H.; Arif, A. M. *Organometallics* **1992**, *11*, 231–237.

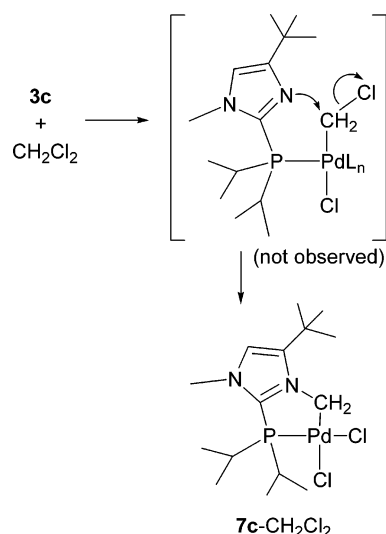
(91) No attempt was made to determine the rotational barriers around the P–imidazole axes because of the complications of simulating spectra containing virtual triplets.

nonchelating phosphine, some without exchange^{92–94} and others with some evidence of exchange.^{95–97} There are examples of other hemilabile Pd complexes, for example ones with pyridylphosphines in which the heterocycle and the phosphine are separated by several atoms,^{98–100} or complexes with phosphines containing ethers¹⁰¹ as well as other functional groups.¹⁰ However, in most cases activation energies were not reported, or in the cases where this information is available,^{99,102} the differences in ligand type or metal preclude any meaningful comparison. Nonetheless, the slightly negative value obtained for ΔS^\ddagger would suggest involvement of either an associative or interchange ligand exchange mechanism rather than a dissociative mechanism via intermediate **B**.

It is surprising that at the low-temperature limit there are four individual proton resonances for each of the four *tert*-butyl substituents; the rotation of the nonchelating phosphine ligand about the Pd–P axis must be hindered by the bulkiness of the *tert*-butyl groups.⁹¹ The situation in the solid (Figure 4) suggests the barrier to rotation in solution.

Because $[\mathbf{6a-Me}]^+[\text{OTf}]^-$ features the same ligand in chelating and nonchelating mode and because it is obvious by looking at NMR data shown in Tables 1 and 2 that there are unusual differences in the NMR data for the same ligand in two coordination modes, a total assignment of all proton and carbon NMR resonances was made using a combination of several experiments. A graphical summary of the results is presented in Supporting Information. HMQC was first used to determine the correlation between proton and carbon, then COSY used to identify which two aromatic protons are in the same imidazole ring, and finally, HMBC was used to locate other pairs of protons and carbons in each imidazole ring. Once the pairs of proton and carbon were divided into two sets, the only question then left was to assign which set belongs to which imidazole, the one on the nonchelating or chelating phosphine. Although it was impossible to ensure this last assignment in the absence of a P–C correlation experiment, it seems reasonable to assign the unusually high-field proton resonance at δ 5.18 ppm to the proton on the unusual ring, the one involved in chelation. The 2D-NMR work assigns this proton as being the one next to nitrogen in the chelating ring. Examination of the solid-state structure (Figure 4) suggests that this proton is shielded by the imidazole ring of the nonchelating ligand. In looking for

Scheme 5



spectroscopic evidence for bonding differences between the two ligands, we note that the magnitude of virtual coupling between imidazole C-2 and the two phosphorus nuclei in the unusual chelate ring is about half that in the nonchelated phosphine ($N = 28.8$ Hz for the signal at 145.8 ppm and 56.5 Hz for the signal at 139.5 ppm).

Reactivity toward Solvents, Particularly CH_2Cl_2 . Both of the Pd(0) complexes **3a**, **3b** were quite stable either in solid state or in the solution, where there was no reaction with solvents such as benzene, dichloromethane, or chloroform. On the other hand, initially colorless solutions of the Pd(0) complex **3c** with less hindered phosphine ligands deposited some dark solid, presumably Pd black, when left at room temperature for a period of weeks. Although the major component was still the Pd(0) complex, some minor unidentified impurities were detected by NMR. In solution of benzene, **3c** was relatively stable, but in dichloromethane, a completely new complex **7c-CH₂Cl₂** was formed (Scheme 5).

Elemental analysis was consistent with the species shown, and the structure of this new complex was confirmed by X-ray diffraction data (Figure 5). The novel square-planar Pd(II) complex bears two chloride ligands and only one phosphine ligand which was alkylated with the CH_2 unit from dichloromethane, resulting in a positive formal charge on the alkylated nitrogen and a formally anionic ligand on Pd. The Pd–P bond length in **7c-CH₂Cl₂** (Table 4, 2.1878 Å) is ca. 0.15 Å shorter than those in **4c-PhI** and **4c-MeOTf**, probably a reflection of the weaker trans influence of chloride in **7c-CH₂Cl₂**. Oxidative additions of dichloromethane to Pd(0) species are known,^{103,104} and the X-ray diffraction structure of $[\text{Cy}_2\text{PCH}_2\text{CH}_2\text{PCy}_2]\text{Pd}(\text{CH}_2\text{Cl})(\text{Cl})$ shows Pd–C = 2.101(9) Å, Pd–P trans to Cl = 2.225(2) and trans to CH_2Cl = 2.317(2) Å, respectively.¹⁰⁴

Another interesting structural feature revealed by the data for Pd–Cl bond lengths in Table 4 is that the Pd–Cl bond trans to phosphine (2.3769 Å) is significantly shorter than the Pd–Cl bond trans to carbon (2.4124 Å).

A likely mechanism for the formation of **7c-CH₂Cl₂** would involve oxidative addition of a C–Cl bond to Pd(0) as suggested

- (92) Farr, J. P.; Olmstead, M. M.; Wood, F.; Balch, A. L. *J. Am. Chem. Soc.* **1983**, *105*, 792–798.
- (93) Jain, V. K.; Jakkal, V. S.; Bohra, R. *J. Organomet. Chem.* **1990**, *389*, 417–426.
- (94) Nicholson, T.; Hirsch-Kuchma, M.; Shellenbarger-Jones, A.; Davison, A.; Jones, A. G. *Inorg. Chim. Acta* **1998**, *267*, 319–322.
- (95) Farr, J. P.; Wood, F. E.; Balch, A. L. *Inorg. Chem.* **1983**, *22*, 2, 3387–3393.
- (96) Suzuki, T.; Kita, M.; Kashiwabara, K.; Fujita, J. *Bull. Chem. Soc. Jpn.* **1990**, *63*, 3434–3442.
- (97) Some examples of fluxionality in pyridylphosphine complexes stem from interchange of two heterocycles attached to the same phosphorus center, for example, in tri(2-pyridyl)- or di(2-pyridyl)phosphines: Wajda-Hermanowicz, K.; Pruchnik, F. P. *Transition Metal Chem. (London)* **1988**, *13*, 101–103. Espinet, P.; Hernando, R.; Iturbe, G.; Villafane, F.; Orpen, A. G.; Pascual, I. *Eur. J. Inorg. Chem.* **2000**, 1031–1038. On some clusters, fluxionality even involves disruption of the pyridylphosphine: Deeming, A. J.; Smith, M. B. *J. Chem. Soc., Chem. Commun.* **1993**, 844–846.
- (98) Hessler, A.; Fischer, J.; Kucken, S.; Stelzer, O. *Chem. Ber.* **1994**, *127*, 481–488.
- (99) Yang, H.; Luga, N.; Mathieu, R. *Organometallics* **1997**, *16*, 2089–2095.
- (100) Del Zotto, A.; Nardin, G.; Rigo, P. *J. Chem. Soc., Dalton Trans.* **1995**, 3343–3351.
- (101) Lindner, E.; Speidel, R.; Fawzi, R.; Iler, W. *Chem. Ber.* **1990**, *123*, 2255–2260.
- (102) Espinet, P.; Hernando, R.; Iturbe, G.; Villafane, F.; Orpen, A. G.; Pascual, I. *Eur. J. Inorg. Chem.* **2000**, 1031–1038.

(103) Leoni, P. *Organometallics* **1993**, *12*, 2432–2434.

(104) Doeiring, A.; Goddard, R.; Hopp, G.; Jolly, P. W.; Kokel, N.; Krueger, C. *Inorg. Chim. Acta* **1994**, *222*, 179–192.

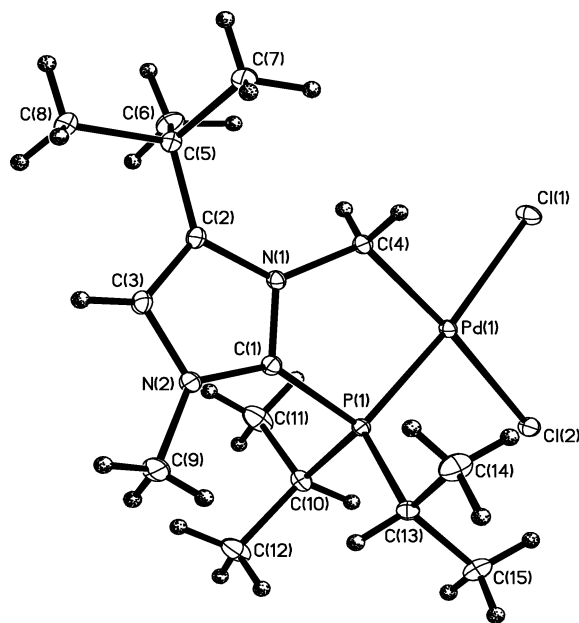


Figure 5. Molecular structure of **7c-CH₂Cl₂**. Ellipsoids are shown at 30% probability.

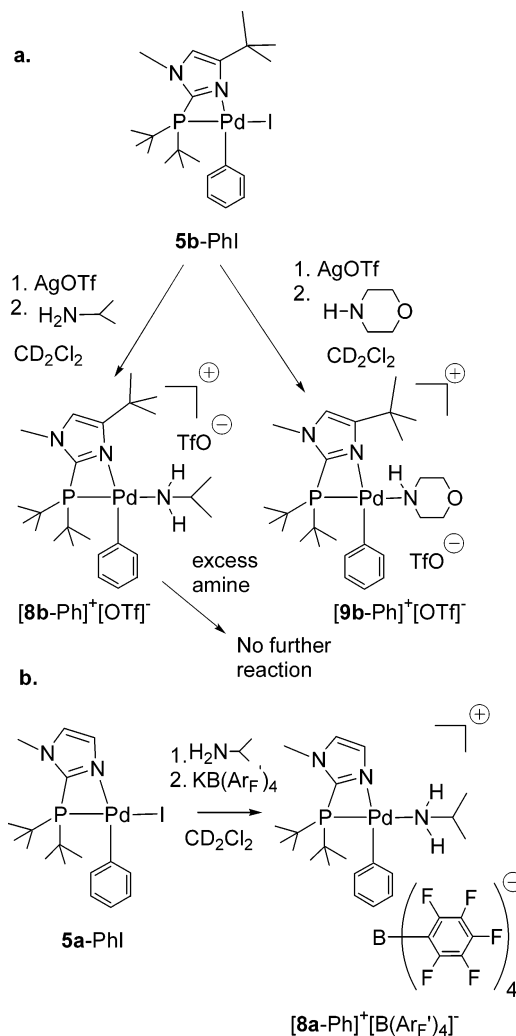
in Scheme 5, followed by displacement of the remaining chloride on carbon by the imidazole nitrogen. It is noteworthy that despite the presence of the large *tert*-butyl group adjacent to nitrogen, attack on the putative Pd–CH₂Cl intermediate seems to occur readily. Formation of **7c-CH₂Cl₂** from **3c** may be considered a bifunctional double activation of the substrate CH₂Cl₂.

In the ¹H NMR spectrum, the most affected resonance is that of the imidazole–H which shifted 1.5 ppm downfield from that of **3c**. Similarly, the resonance for protons of the isopropyl substituents on phosphorus shifted downfield, whereas the peaks for the methyl hydrogens on the isopropyl substituents appear as two doublet of doublets because the methyl groups are diastereotopic. These chemical shift changes may be due to the two new trans ligands (chlorides) as well as alkylation of the imidazole ring, which changes the distribution of the formal charge on the aromatic ring.

Addition of Amines or Other Polar Ligands to Chelated Oxidative Addition Products without Opening of the Chelate. In the process of coupling between aryl halides and amines, the step which follows oxidative addition is believed to be coordination of the amine to an open site on the Pd center. Although there was no open site on complexes **5a-PhX** and **5b-PhI**, our expectation was that the chelate ring would open, with the amine nitrogen coordinating to Pd. We expected that this process would be facilitated not only by relief of any strain in the chelate but also by hydrogen bonding between one of the N–H bonds of the coordinated amine and the now-free imidazole nitrogen, an interaction we saw between coordinated water and imidazole substituent in Ru complex **1**.⁷⁵

Surprisingly, in **5a-PhX** (X = Br, I) and **5b-PhI** the chelate ring stayed closed when primary and secondary amines were added; no binding of amine was detected as evidenced by lack of changes in ¹H or ³¹P NMR spectral data. The same result was obtained when H₂O was added. Similarly, when complex **[6a-Me]⁺[OTf][–]** was treated individually with isopropylamine, water, or 2-propanol, the chelate ring stayed closed also, and if any coordination of the ligands took place, it was to an undetectable extent.

Scheme 6. Amine Binding without Chelate Opening



One way of opening a coordination site in a halopalladium complex would be to abstract halide ion. Thus, the oxidative addition product with one chelating phosphine ligand **5b-PhI** was ionized by silver triflate in dichloromethane (Scheme 6), forming a yellow precipitate assumed to be silver iodide. After the yellow precipitate was removed, one equivalent of the primary amine, isopropylamine was added to the filtrate. The ³¹P{¹H} NMR spectrum showed there was only one major species in the NMR solution. After isolation, purification, and characterization, the product was found to be **[8b-Ph]⁺[OTf][–]** (Scheme 6a). The elemental analysis data were consistent with the formula (phosphine)Pd(Ph)(isopropylamine)(triflate). The strong absorption at 1270 cm^{–1} indicated the S–O stretch in the free triflate ion. A square-planar Pd(II) cation in this formula would reasonably contain a chelated phosphine in addition to phenyl and amine ligands. The NMR data were consistent with this structure though not diagnostic. In the ¹H NMR spectrum, the resonance for the N–H protons in isopropylamine appeared at 2.83 ppm as a slightly broad singlet, whereas in the ³¹P{¹H} NMR spectrum, the singlet at +39.8 ppm was shifted 10 ppm downfield from that of **5b-PhI**, either because of the change of the trans ligand to the phosphorus atom or the overall charge on the metal. We could not tell the precise bonding in the product from the spectral data, but the molecular structure was clarified by X-ray diffraction. The crystal structure shown in

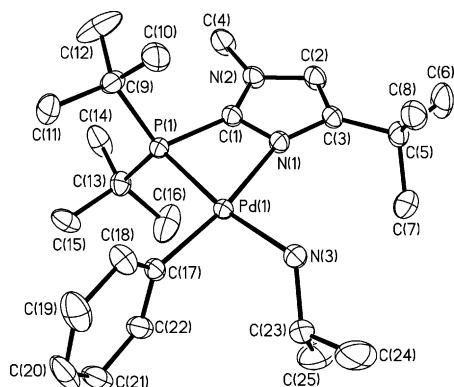


Figure 6. Molecular structure of $[8b-Ph]^+[OTf]^-$. Only the cation is shown. Ellipsoids are shown at 30% probability.

Figure 6 demonstrated the binding of isopropylamine, where the Pd–N bond length [Table 4, 2.129(2) Å] falls in the range of that in Pd complex with bound amine.^{105,106} Looking at Table 4, it is interesting to compare the structures of **5b-PhI** and **[8b-Ph]⁺OTf[−]**: in going from the neutral to the ionic species, the Pd–P(1) and Pd–N(Im) bond lengths decrease by 0.025(1) and 0.065(4) Å, respectively, with a concomitant increase in the P(1)–Pd–N(Im) angle of 1.1(1)°. The four interligand bond angles shown in Table 4 change by at most 2.4°, with θ_1 and θ_2 together increasing by a total of 3.5° and the opposite angles θ_3 and θ_4 together decreasing by the same amount. These changes may reflect both the increase in positive charge on the complex (tightening the chelate) and the reduced size of the ligand cis to phenyl (from I to H₂NR). Since amine and phenyl ligands are located cis to each other, the release of arylated amine through reductive elimination is conceivable. However, the addition of excess amine to pure **[8b-Ph]⁺OTf[−]** did not open the chelate ring.

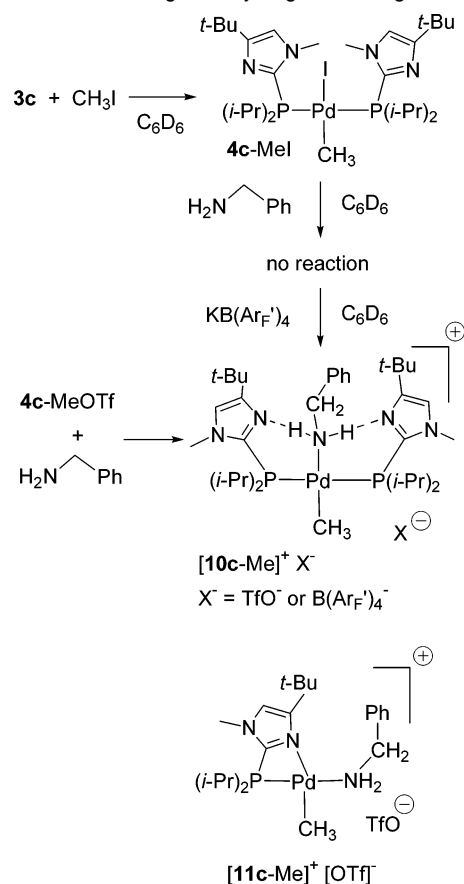
A product with similar spectral data was obtained when the secondary amine morpholine was used instead of isopropylamine to react with **5b-PhI** and silver triflate (Scheme 6a), so that we assume a similar structure, **[9b-Ph]⁺OTf[−]**.

The analogous reaction with **5a-PhI** gave slightly different results. The use of ionizing agent, silver triflate, and the subsequent addition of amine yielded a mixture with many minor species. However, when the ionizing reagent was changed to potassium tetrakis(pentafluorophenyl)borate [KB(ArF')₄] and amine was added prior to the addition of ionizing reagent, the reaction was cleaner, with a major species assigned structure **[8a-Ph]⁺[B(ArF')₄][−]** on the basis of spectral data similar to those of **[8b-Ph]⁺OTf[−]** (Scheme 6b).

In summary, the products from the reactions between **5a-PhI**, **5b-PhI** with ionizing reagents and amine had very similar structures. In the resulting complexes, the amine coordinated to Pd as a neutral ligand, oriented cis to the phenyl ligand. In the case of **5a-PhI**, the sequence of adding ionizing reagents and amine was essential, and the choice of ionizing reagent was important also.

Binding of Amines with Hydrogen Bonding. Whereas **[6a-Me]⁺OTf[−]** did not react with an amine, neutral but less

Scheme 7. Amine Binding with Hydrogen Bonding



hindered **4c-MeOTf** did react with benzylamine to give an ionic product in which the weakly coordinating triflate ion was replaced by the amine (Scheme 7). When the amine binding reaction was carried out in dichloromethane, only **[10c-Me]⁺OTf[−]** was observed and isolated. IR absorption suggested an ionic triflate rather than bound triflate, but ultimately X-ray diffraction was used to verify the structure (see below). Interestingly, when the reaction of **4c-MeOTf** and benzylamine was carried out in C₆D₆, a mixture containing four species was observed, three being unreacted **4c-MeOTf**, free phosphine **2c**, and **[10c-Me]⁺OTf[−]** as shown by ³¹P{¹H} NMR peaks at δ 24.4, −17.7, and 28.6 ppm, respectively. The appearance of free ligand **2c** and the fourth species (³¹P{¹H} NMR δ 33.4 ppm) in a molar ratio of approximately 1 to 1 suggests that the latter compound is the monophosphine complex **[11c-Me]⁺OTf[−]**, though we were unable to isolate it from this mixture and it was not characterized further. The nature of hydrogen bonding in purified **[10c-Me]⁺OTf[−]** was not clearly revealed in its infrared spectrum, which exhibited several weak bands in the region 3000–3400 cm^{−1}.

Therefore, crystals of **[10c-Me]⁺OTf[−]** were grown for X-ray diffraction study, the results of which are shown in Figure 7. The two phosphine ligands are located trans to each other, and the benzylamine is coordinated to Pd trans to the methyl ligand. Significantly, the benzylamine fits into a binding pocket created by the two heterocyclic phosphine ligands acting as hydrogen-bond acceptors to the amine. The distances between the amine hydrogens and the interacting nitrogens on the imidazole rings were 2.05 and 2.09 Å which was in the range of N–H distance involved in hydrogen bonding.¹⁰⁷

(105) Kumar, J. S.; Singh, A. K.; Yang, J.; Drake, J. E. *J. Coord. Chem.* **1998**, *44*, 217–223.

(106) Zhao, G.; Lina, H.; Yub, P.; Suna, H.; Zhua, S.; Sua, X.; Chen, Y. *J. Inorg. Biochem.* **1999**, *73*, 145–149.

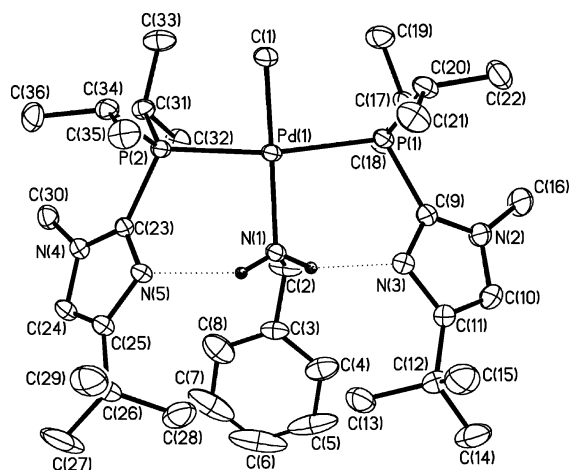


Figure 7. Molecular structure of the cation of $[10c\text{-Me}]^+[\text{OTf}]^-$. Ellipsoids are shown at 30% probability.

The same cation could be created in three steps, first by performing oxidative addition of iodomethane to **3c** to give **4c-MeI**, in a fast and clean reaction like that with iodobenzene. Subsequent addition of benzylamine followed by of potassium tetra(pentafluorophenyl)borate resulted in the formation of $[10c\text{-Me}]^+[\text{B}(\text{Ar}_F)_4]^-$ (Scheme 7). The X-ray crystal structure of this complex obtained from $\text{Et}_2\text{O}/\text{CH}_2\text{Cl}_2$ (shown in Supporting Information) also showed a hydrogen bond between each amine N-H and the nitrogen atom on closest imidazole ring. The only difference between $[10c\text{-Me}]^+[\text{OTf}]^-$ and $[10c\text{-Me}]^+[\text{B}(\text{Ar}_F)_4]^-$ is the anion; thus, the corresponding bond lengths and bond angles are comparable (Table 4).

Conclusion

A series of three new imidazolylphosphine ligands was designed and synthesized to probe the effects of phosphorus and heterocycle substituents on coordination geometry and ligand hapticity in $\text{Pd}(0)$ and $\text{Pd}(\text{II})$ complexes of these ligands. In verification of the HSAB concept,⁴⁸ the X-ray diffraction and spectroscopic data for $\text{Pd}(0)$ complex **3a** show that it is a two-coordinate, 12-electron species despite the availability of the heterocyclic nitrogens to enter into chelation and the proximity of hydrogens on the *N*-methyl groups to enter into agostic interactions.

Oxidative addition chemistry of the two-coordinate $\text{Pd}(0)$ complexes **3a–3c** shows that isopropyl substituents not only allow rapid reaction but also retention of both phosphine ligands in **4c-PhI** and **4c-MeOTf**. In contrast, phosphorus *tert*-butyl groups slow oxidative addition and lead to phosphine loss and chelation by the remaining phosphine in **5a-PhBr**, **5a-PhI**, and **5b-PhI**. Unlike isopropyl-substituted complex **4c-MeOTf**, which features a metal-bound triflate ion, *tert*-butyl-substituted analogue $[6a\text{-Me}]^+[\text{OTf}]^-$ is ionic because the triflate ligand has been displaced by one imidazole nitrogen in forming a chelate. Taken together, these results show a strong enforcement of chelation by larger substituents *R* in $\text{R}_2\text{PR}'$ ($\text{R}' = \text{imidazol-2-yl}$). This preference is reminiscent of the trends noted in the past for metalation of R' when *R* is large. Comparing **5a-PhI** and **5b-PhI** one can see the effects of increasing steric hindrance at the chelating imidazole nitrogen, notably a lengthening of

the $\text{Pd-N}(\text{Im})$ bond, yet this is insufficient to allow opening of the chelate by amines. In fact, in all of the di-*tert*-butylphosphino-substituted compounds in this study, the chelate remained closed when amines were added. Amine binding could be effected after halide ionization but without opening of the chelate ring in $[8b\text{-Ph}]^+[\text{OTf}]^-$, $[9b\text{-Ph}]^+[\text{OTf}]^-$, and $[8a\text{-Ph}]^+[\text{OTf}]^-$. Amine binding involving hydrogen bonding was seen in the isopropyl series by looking at the crystal structures of $[10c\text{-Me}]^+[\text{OTf}]^-$ and its $[\text{B}(\text{Ar}_F)_4]^-$ analogue. The results described here show the interplay of ligand substituents in determining ligand hapticity, coordination of other ligands, and secondary hydrogen-bonding interactions, properties of interest in studying structure and catalysis of complexes featuring hybrid ligands.

Experimental

General Information. Reactions were performed under dry nitrogen, using a combination of Schlenk line and glovebox techniques. C_6D_6 was distilled from LiAlH_4 prior to use, and CDCl_3 was distilled from CaH_2 . NMR tube reactions were performed in resealable NMR tubes (J. Young).

Unless otherwise specified, ^1H and ^{13}C data were measured at 30 °C on a 500 MHz (499.9 MHz for ^1H and 125.7 MHz for ^{13}C) and ^{31}P data were measured on a 200 MHz (80.95 MHz for ^{31}P) spectrometer. ^1H and ^{13}C NMR chemical shifts are reported in ppm downfield from tetramethylsilane and referenced to solvent resonances (^1H NMR: δ 7.16 for C_6HD_5 , δ 7.27 for CHCl_3 , 5.32 for CHD_2Cl_2 and ^{13}C NMR: δ 128.39 for C_6D_6 , δ 77.23 for CDCl_3 , 54.00 for CD_2Cl_2). ^1H NMR signals are given followed by multiplicity, coupling constants *J* in Hertz, integration in parentheses. For complex coupling patterns, the first coupling constant listed corresponds to the first splitting listed, e.g. for (dt, $J = 3.2, 7.9, 1$ Hz) the doublet exhibits the 3.2-Hz coupling constant. $^{31}\text{P}\{^1\text{H}\}$ NMR chemical shifts are referenced to an external 85% H_3PO_4 (aq) capillary placed in the solvent. IR spectra at ambient temperatures were obtained on a ThermoNicolet Nexus 670 FT-IR spectrometer. Samples were examined in C_6D_6 or CD_2Cl_2 solution in NaCl cells. Elemental analyses were performed at NuMega Laboratories in San Diego, CA, for the Pd complexes and by Desert Analytics, Tucson, AZ, for the ligands. Electrospray mass spectra were obtained on a Finnigan LCQ spectrometer.

Crystallographic Work. Data relating to the X-ray structural determinations are collected in Table 5. All data were collected on Bruker diffractometers equipped with APEX CCD detectors. All structures were solved by direct methods and refined with anisotropic thermal parameters and idealized hydrogen atoms. All software is contained in the SMART, SAINT, and SHELXL libraries distributed by Bruker-AXS (Madison, WI). Complete disclosures about the crystallographic work may be found in the CIF files in Supporting Information.

Preparation of Di-*tert*-butyl-(1-methyl-imidazol-2-yl)phosphine (2a). A 50-mL Schlenk flask containing a stir bar was charged with redistilled 1-methylimidazole (1.18 g, 0.014 mol) and dry, deoxygenated THF (20 mL). The reaction solution was cooled to -78 °C. A 1.6 M solution of *n*-BuLi (9.0 mL, 0.014 mol) was added dropwise, and the reaction was allowed to stir at -78 °C. After 0.5 h, di-*tert*-butylchlorophosphine (2.57 g, 0.014 mol) was added dropwise. The reaction was stirred at -78 °C for 0.5 h before warming up to room temperature overnight. Deoxygenated methanol (5 mL) was added, and solvents were removed on a vacuum line. Petroleum ether was added to the solid; the mixture was stirred and filtered through Celite under nitrogen. The filtrate was concentrated to a small volume (about 4 mL) and purified by radial chromatography on a 4-mm silica plate under nitrogen with hexane/ethyl acetate (8:2). The high *R_f* fraction was collected and the solvent was removed on vacuum line. Pure **2a** was obtained as clear viscous oil (2.30 g, 74%). Anal. Calcd for $\text{C}_{12}\text{H}_{23}\text{N}_2\text{P}$ (226.30): C, 63.69; H, 10.24; N, 12.38. Found C, 63.71; H, 10.28; N, 12.34.

(107) Jeffery, G. A. *An Introduction to Hydrogen Bonding*; Oxford: New York, 1997.

Table 5. Collection Data for Crystal Structures of the Complexes

	3a	4c-MeOTf	4c-PhI	5a-PhBr	5a-PhI	5b-PhI	7c-CH ₂ Cl ₂	[8b-PhI][OTf]–	[10c-MeI][OTf]–	[10c-MeI][B(Ar _F) ₄]–
formula	C ₃₄ H ₆₀ N ₄ P ₂ Pd	C ₃₀ H ₅₇ F ₃ N ₄ O ₃ P ₂ PdS	C ₃₄ H ₅₉ IN ₄ P ₂ Pd	C ₁₈ H ₂₈ BrN ₂ PPd	C ₁₈ H ₂₈ IN ₂ PPd	C ₂ H ₃₆ IN ₂ PPd	C ₃₀ H ₃₆ Cl ₂ N ₂ P ₂ Pd	C ₃₆ H ₄₈ F ₃ N ₃ O ₃ PPdS	C ₃₇ H ₆₀ F ₃ N ₃ O ₃ P ₂ PdS	C ₆₀ H ₆₀ BF ₂ ON ₃ P ₂ Pd
<i>M_w</i>	558.99	779.24	819.09	489.70	536.69	592.80	445.67	674.08	885.33	1416.33
crystal system	monoclinic	orthorhombic	monoclinic	monoclinic	monoclinic	monoclinic	monoclinic	triclinic	triclinic	monoclinic
space group	<i>P</i> ₂ / <i>1</i> / <i>n</i>	<i>P</i> ₂ ₁ <i>2</i> ₁ <i>2</i> ₁	<i>P</i> ₂ / <i>1</i> / <i>c</i>	<i>P</i> ₂ / <i>1</i> / <i>n</i>	<i>P</i> ₂ / <i>1</i> / <i>n</i>	<i>P</i> ₂ / <i>1</i> / <i>n</i>	<i>P</i> ₂ / <i>1</i> / <i>n</i>	<i>P</i> ₁	<i>P</i> ₁	<i>P</i> ₂ / <i>1</i> / <i>n</i>
crystal dim (mm)	0.3×0.3×0.25	0.30×0.25×0.15	0.40×0.15×0.08	0.40×0.30×0.10	0.50×0.25×0.10	0.35×0.30×0.15	0.20×0.15×0.10	0.32×0.30×0.15	0.40×0.35×0.30	0.28×0.08×0.07
color	colorless	colorless	colorless	colorless	colorless	colorless	yellow	yellow	colorless	colorless
<i>a</i> [Å]	15.9009	9.6134	14.3428	9.5657	9.9008	10.3039	9.9919	10.7472	13.2846	23.6456
<i>b</i> [Å]	11.4188	16.0484	10.4371	16.3449	16.7186	20.2485	17.5170	11.485	13.6817	9.9940
<i>c</i> [Å]	16.5897	25.4098	26.6199	12.8255	12.9150	12.1211	11.0258	14.9802	13.7439	26.4930
<i>α</i> [deg]	90	90	90	90	90	90	90	90	90	90
<i>β</i> [deg]	110.4000	90	97.0240	99.8240	102.8490	103.8140	98.5320	83.3990	109.5820	96.8290
<i>γ</i> [deg]	90	90	90	90	90	90	90	62.8250	105.1180	90
<i>V</i> [Å ³]	2823.3	3920.2	3955.0	1975.9	2084.26	2455.8	1908.47	1615.80	2254.2	6216.3
<i>Z</i>	4	4	4	4	4	4	4	2	2	4
<i>D</i> _{calcd} (g cm ^{−3})	1.315		1.376	1.646	1.710	1.603				1.513
<i>λ</i> [Å]	0.71073	0.71070	0.71047	0.71076	0.71108	0.71073	0.71067	0.70964	0.71073	0.71077
<i>T</i> [K]	223	100	218	147	147	150	150	218	213	100
<i>2θ</i> _{max} [deg]	28.27	27.50	28.15	28.30	28.26	28.25	28.27	28.29		26.00
measured reflns.	20705	23881	28863	12128	12908	14972	11711	10107	15104	12187
independent reflns.	6800	8900	9506	4542	4808	5592	4395	6661	8765	9499
no. of params.	280	626	398	208	208	244	306	523		827
<i>R</i> (<i>F</i>)	2.78	2.59	3.88	2.73	2.30	2.32	2.11	3.38		4.32
(<i>I</i> > 2σ(<i>I</i>)), % ^a	9.47	6.02	9.20	7.12	5.88	5.84	5.25	8.76	10.39	8.77
<i>R</i> (<i>wF</i> ²)										
(<i>I</i> > 2σ(<i>I</i>)), % ^b										
GOF	1.069	1.099	1.028	1.079	1.022	1.045	1.050	1.001		1.027
res. electron density	0.836	0.650	0.235	0.864	1.129	0.700	0.647	0.622		0.615

$$^a R = \sum |F_o| - |F_c| / \sum |F_o|, \quad ^b R(wF^2) = \{ \sum [\omega(F_o^2 - F_c^2)^2] / \sum [\omega(F_o^2)^2] \}^{1/2}, \quad \omega = 1/[\sigma^2(F_o^2) + (aP)^2 + bP], \quad P = [2F_c^2 + \max(F_o, 0)]/3.$$

Preparation of Di-*tert*-butyl-(4-*tert*-butyl-1-methyl-imidazol-2-yl)-phosphine (2b). A 100-mL Schlenk flask was charged with 4-*tert*-butyl-1-methylimidazole¹⁰⁸ (3.17 g, 0.023 mol) and dry and deoxygenated THF (25 mL), and the resulting solution was cooled to -78°C using a dry ice/acetone bath. A 1.6 M solution of *n*-BuLi (13.7 mL, 0.022 mol) was added dropwise over 3 min. The reaction solution was stirred at -78°C . After 2 h, di-*tert*-butylchlorophosphine (4.28 g, 0.024 mol) was added dropwise. The solution was stirred at -78°C for 0.5 h and then allowed to warm to room temperature overnight. The solution was quenched with deoxygenated methanol (5 mL). Solvents were removed on a vacuum line, and the resulting solid was suspended in deoxygenated petroleum ether and filtered through Celite under nitrogen. The filtrate was concentrated to a small volume (5 mL) and chilled to -50°C . Colorless crystals of **2b** were obtained by removing the supernatant with a pipet and washing with cold petroleum ether and storing the product on a vacuum line (5.20 g, 81%). Mp $50\text{--}51^{\circ}\text{C}$. Anal. Calcd for $\text{C}_{16}\text{H}_{31}\text{N}_2\text{P}$ (282.40): C, 68.05; H, 11.07; N, 9.92. Found C, 67.86; H, 11.11; N, 9.81.

Preparation of Di-isopropyl(4-*tert*-butyl-1-methyl-imidazol-2-yl)-phosphine (2c). To a stirred solution of 4-*tert*-butyl-1-methyl-imidazole (2.87 g, 0.021 mol) in dry and deoxygenated THF (25 mL) a 1.6 M solution of *n*-BuLi (13.0 mL, 0.021 mol) was added dropwise at room temperature. After 1 h, the solution was cooled to -78°C , and a solution of di-isopropylchlorophosphine (3.09 g, 0.020 mol) in THF (5 mL) was added dropwise. The solution was allowed to warm to room temperature and stir for 2 h. The solution was then quenched with deoxygenated methanol (5 mL). Solvents were removed on a vacuum line, and the resulting solid was suspended in deoxygenated petroleum ether and filtered through Celite under nitrogen. The filtrate was concentrated and purified by radial chromatography on a 4-mm silica plate under nitrogen with hexane/ethyl acetate (9:1). The high R_f fraction was collected, and the solvent was removed on a vacuum line. Pure **2c** was obtained as a clear oil (3.74 g, 73%). Anal. Calcd for $\text{C}_{14}\text{H}_{27}\text{N}_2\text{P}$ (254.35): C, 66.11; H, 10.70; N, 11.01. Found C, 65.49; H, 10.45; N, 10.50.

Preparation of Bis(di-*tert*-butyl-1-methylimidazol-2-yl-phosphine)-palladium (0) (3a). Di-*tert*-butyl-1-methyl-imidazol-2-ylphosphine **2a** (290.4 mg, 1.28 mmol) was added to a reaction vial containing Cp-(allyl)Pd (136 mg, 0.64 mmol) and a magnetic stir bar. Deoxygenated and dry benzene (5 mL) was added to afford a dark-red solution. After stirring at room temperature for 2 d, solvent was removed. The resulting residue was redissolved in THF/hexanes (about 1 mL) and filtered. The filtrate was stored in a vial at -50°C . After 24 h, the cold supernatant was removed, and the colorless crystals were washed with cold hexane and dried to give **3a** (305 mg, 85%). Anal. Calcd for $\text{C}_{24}\text{H}_{46}\text{N}_4\text{P}_2\text{Pd}$ (559.03): C, 51.55; H, 8.29; N, 10.02. Found: C, 51.63; H, 8.00; N, 9.98. IR (C_6D_6): $2956\text{ (m)}\text{ cm}^{-1}$.

Preparation of Bis(di-*tert*-butyl-1-methyl-4-*tert*-butyl-imidazol-2-yl-phosphine)palladium (0) (3b). Di-*tert*-butyl-1-methyl-4-*tert*-butyl-imidazol-2-yl-phosphine **2b** (440 mg, 1.56 mmol) was added to a reaction vial containing Cp(allyl)Pd (154 mg, 0.72 mmol) and a magnetic stir bar. Deoxygenated and dry benzene (8 mL) was added to afford a dark-red solution which was allowed to stir at room temperature. After 2 d, solvent was removed, and the residue was redissolved in hexane (about 2 mL). After filtration, the filtrate was stored at -50°C . After 24 h, the cold supernatant was removed, and the colorless crystals were washed with cold hexane and dried to give **3b** (278 mg, 62%). Anal. Calcd for $\text{C}_{32}\text{H}_{62}\text{N}_4\text{P}_2\text{Pd}$ (671.24): C, 57.26; H, 9.31; N, 8.35. Found: C, 57.33; H, 9.08; N, 8.41. IR (C_6D_6): $2959\text{ (m)}\text{ cm}^{-1}$.

Synthesis of Bis(di-isopropyl-1-methyl-4-*tert*-butylimidazol-2-yl-phosphine)Pd(0) (3c). Di-isopropyl-1-methyl-4-*tert*-butylimidazol-2-yl-phosphine **2c** (493 mg, 1.94 mmol) was transferred to a reaction vial equipped with magnetic stir bar. Cp(allyl)Pd (192 mg, 0.90 mmol)

was then added followed by deoxygenated benzene (8 mL). The resulting dark-red solution was allowed to stir at room temperature. After 2 d, the reaction was stopped, and the pale orange solution was concentrated to dryness. The residue was redissolved in hot THF/hexanes (approximately 1.5 mL) and then chilled to -50°C . After 24 h, the cold supernatant was removed by pipet, and the colorless crystals were washed with cold hexane and dried under vacuum to give **3c** (454 mg, 82%) pure by NMR spectroscopic analysis. Anal. Calcd for $\text{C}_{28}\text{H}_{54}\text{N}_4\text{P}_2\text{Pd}$ (615.12): C, 54.67; H, 8.85; N, 9.11. Found: C, 52.08; H, 8.53; N, 8.74. IR (C_6D_6): $2955\text{ (m)}, 2276\text{ (m)}\text{ cm}^{-1}$.

Preparation of *trans*-Bis(di-isopropyl-1-methyl-4-*tert*-butyl-imidazol-2-yl-phosphine)Pd(Ph)(I) (4c-PhI). In a reaction vial, **3c** (156 mg, 0.254 mmol) was weighed, and then deoxygenated benzene (2 mL) was added. The reaction vial was shaken to allow everything to dissolve, and a homogeneous solution was obtained. Iodobenzene (58.3 mg, 0.286 mmol) was then added via syringe. The yellow solution was allowed to stir at room temperature. After 2 d, solvent was removed, and the crude product was recrystallized by slowly diffusing hexane into a benzene solution to give yellow crystals (147 mg, 71%). Anal. Calcd for $\text{C}_{34}\text{H}_{59}\text{IN}_4\text{P}_2\text{Pd}$ (819.15): C, 49.85; H, 7.26; N, 6.84. Found: C, 49.52; H, 7.06; N, 6.85. IR (CDCl_3): $2963\text{ (s)}, 1562\text{ (s)}, 1470\text{ (s)}\text{ cm}^{-1}$.

Preparation of *trans*-Bis(di-isopropyl-1-methyl-4-*tert*-butyl-imidazol-2-ylphosphine)Pd(CH_3)(OTf) (4c-MeOTf). Palladium (0) complex **3c** (73.4 mg, 0.119 mmol) and deoxygenated benzene (3 mL) were added to a reaction vial equipped with a magnetic stir bar. Methyl triflate (23.2 mg, 0.141 mmol) was added via syringe to give a slightly yellow-colored solution. After being stirred at room temperature for 1 d, solvent was removed, and the solid residue was recrystallized by slowly diffusing hexane into a benzene solution. Yellow crystals (57.5 mg, 62%) were then obtained after washing and drying. Anal. Calcd for $\text{C}_{30}\text{H}_{57}\text{F}_3\text{N}_4\text{O}_3\text{P}_2\text{PdS}$ (779.24): C, 46.24; H, 7.37; N, 7.19. Found: C, 46.63; 6.98; 7.16. IR (C_6D_6): $2961\text{ (s)}, 1315\text{ (s)}\text{ cm}^{-1}$.

Synthesis of (Di-*tert*-butyl-1-methylimidazol-2-yl-phosphine)Pd-(Ph)(I) (5a-PhI). In a reaction vial, **3a** (148 mg, 0.265 mmol) was weighed, and then deoxygenated benzene (3 mL) was added. The reaction vial was shaken to allow everything to dissolve, and a homogeneous solution was obtained. Iodobenzene (52.8 mg, 0.259 mmol) was then added via syringe. The resulting solution was mixed and allowed to stand still at room temperature for 24 h. The yellow crystals which formed were isolated by removing the mother liquor using a pipet, washing with benzene and drying under vacuum (134 mg, 94%). Anal. Calcd for $\text{C}_{18}\text{H}_{28}\text{IN}_2\text{PPd}$ (536.73): C, 40.28; H, 5.26; N, 5.22. Found: C, 40.52; H, 5.04; N, 5.31. IR (CH_2Cl_2): $2967\text{ (s)}, 1712\text{ (s)}, 1562\text{ (s)}, 1470\text{ (s)}\text{ cm}^{-1}$.

Preparation of (Di-*tert*-butyl-1-methyl-imidazolylphosphine)Pd-(Ph)(Br) (5a-PhBr). In a reaction vial, **3a** (42.7 mg, 0.076 mmol) was weighed, and then deoxygenated benzene (1 mL) was added. The reaction vial was shaken to allow everything to dissolve, and a homogeneous solution was obtained. Bromobenzene (11.9 mg, 0.076 mmol) was then added via syringe. The resulting solution was mixed and allowed to stand still at room temperature for 24 h. The yellow crystals which formed were isolated by removing the mother liquor using a pipet, washing with benzene, and drying under vacuum (25 mg, 72%). Anal. Calcd for $\text{C}_{18}\text{H}_{28}\text{BrN}_2\text{PPd}$ (489.73): C, 44.15; H, 5.76; N, 5.72. Found: C, 44.14; H, 5.64; N, 5.77. IR (CH_2Cl_2): $2927\text{ (s)}, 1563\text{ (s)}, 1471\text{ (s)}\text{ cm}^{-1}$.

Preparation of (Di-*tert*-butyl-1-methyl-4-*tert*-butyl-imidazol-2-ylphosphine)Pd(Ph)(I) (5b-PhI). In a reaction vial, **3b** (121 mg, 0.180 mmol) was weighed. Then deoxygenated benzene (2 mL) was added. The reaction vial was shaken to allow everything to dissolve and a homogeneous solution was obtained. Iodobenzene (36.5 mg, 0.178 mmol) was then added via syringe. The resulting solution was mixed and allowed to stand still at room temperature for 24 h. The yellow crystals which formed were isolated by removing the mother liquor using a pipet, washing with benzene, and drying under vacuum (104 mg, 97%). Anal. Calcd for $\text{C}_{22}\text{H}_{36}\text{IN}_2\text{PPd}$ (592.83): C, 44.57; H, 6.12;

(108) Lipshutz, B. H.; Morey, M. C. *J. Org. Chem.* **1983**, *48*, 3745–3750.

N, 4.73. Found: C, 44.26; H, 5.90; N, 4.76. IR (CDCl₃): 2963 (s), 1562 (s), 1470 (s) cm⁻¹.

Synthesis of (Di-*tert*-butyl-1-methylimidazol-2-ylphosphine)Pd-(CH₃)[OTf] ([6a-Me]⁺[OTf]⁻). Palladium(0) complex **3a** (76.8 mg, 0.137 mmol) and deoxygenated benzene (3 mL) were added to a reaction vial equipped with magnetic stir bar. Methyl triflate (22.5 mg, 0.137 mmol) was added via syringe to give a slightly yellow-colored solution. After being stirred at room temperature for 1 d, solvent was removed, and the resulting solid was recrystallized by slowly diffusing diethyl ether into a dichloromethane solution. Colorless crystals (65.7 mg, 66%) were then obtained. Anal. Calcd for C₂₅H₄₉F₃N₄O₃P₂PdS (723.18): C, 43.18; H, 6.83; N, 7.74. Found: C, 43.11; H, 7.13; N, 7.85. IR (CDCl₃): 1270 (s) cm⁻¹.

Preparation of (Di-isopropyl-1-methyl-3-methylene-4-*tert*-butyl-imidazol-2-ylphosphine)PdCl₂ (7c-CH₂Cl₂). Palladium (0) complex **3c** (33.3 mg, 0.054 mmol) was dissolved in a vial using dry and deoxygenated dichloromethane (2 mL). The resulting yellow solution was allowed to stir at room temperature. After 24 h, the reaction solution was concentrated to one-third of the original volume, and diethyl ether was slowly diffused into the solution. White crystals (19.2 mg, 79.8%) were so obtained. Anal. Calcd for C₁₅H₂₉Cl₂N₂PPd (445.70): C, 40.42; H, 6.56; N, 6.29. Found: C, 40.24; H, 6.50; N, 6.58. IR (CD₂Cl₂): 2970 (m), 2298 (w), 1712 (s) cm⁻¹.

Preparation of (Di-*tert*-butyl-1-methyl-4-*tert*-butyl-imidazol-2-ylphosphine)Pd(Ph)(NH₂CH(CH₃)₂)[OTf] ([8b-Ph]⁺[OTf]⁻). Complex **5b-PhI** (46.0 mg, 0.077 mmol) was transferred to a vial containing silver triflate (21.2 mg, 0.083 mmol). Degassed dichloromethane was added followed by isopropylamine (6.25 mg, 0.106 mmol). The reaction mixture was shaken, and a yellow precipitate formed right away. The upper colorless solution was isolated by filtering the suspension through cotton and Celite. The filtrate was then concentrated down to a small volume, and diethyl ether was allowed to diffuse into it to give colorless crystals (22.6 mg, 56%). Anal. Calcd for C₂₆H₄₅F₃N₃O₃PPdS (674.12): C, 46.32; H, 6.73; N, 6.23. Found: C, 46.10; H, 6.95; N, 6.22. IR (CD₂Cl₂): 3327 (w), 2971 (m), 1566 (m), 1270 (s) cm⁻¹.

Preparation of (Di-*tert*-butyl-1-methyl-4-*tert*-butyl-imidazol-2-ylphosphine)Pd(Ph)(morpholine)[OTf] ([9b-Ph]⁺[OTf]⁻). Complex **5b-PhI** (21.9 mg, 0.037 mmol) was transferred to a vial containing silver triflate (12.1 mg, 0.047 mmol). Degassed dichloromethane was added followed by the addition of morpholine (9.99 mg, 0.115 mmol). The reaction mixture was shaken, and a yellow precipitate formed right away. The upper colorless solution was isolated by filtering the suspension through cotton and Celite. The filtrate was then concentrated down to a small volume, and diethyl ether was allowed to diffuse into it to give colorless crystals (15.6 mg, 76%). Anal. Calcd for C₂₇H₄₅F₃N₃O₄PPdS (702.12): C, 46.19; H, 6.46; N, 5.98. Found: C, 42.51; H, 5.56; N, 6.15. Anal. Calcd for C₂₇H₄₅F₃N₃O₄PPdS + CH₂-

Cl₂ (702.12 + 84.93): C, 42.73; H, 6.02; N, 5.34. IR (CD₂Cl₂): 2970 (m), 1565 (m), 1271 (s) cm⁻¹.

Preparation of *trans*-Bis(di-isopropyl-1-methyl-4-*tert*-butyl-imidazol-2-ylphosphine)₂Pd(CH₃)(NH₂CH₂Ph)[OTf] ([10c-Me]⁺[OTf]⁻). Complex **4c-MeOTf** (36.0 mg, 0.058 mmol) was dissolved in dichloromethane (1 mL) to give a clear solution. Benzylamine (6.27 mg, 0.058 mmol) was added via syringe. The reaction mixture was allowed to stir at room temperature. After 24 h, the solution was concentrated to dryness, and the resulting solid was recrystallized by slowly diffusing diethyl ether into a dichloromethane solution. The colorless crystals were washed with cold diethyl ether and dried under vacuum (33.7 mg, 65%). Anal. Calcd for C₃₇H₆₆F₃N₅O₃P₂PdS (885.33): C, 50.14; H, 7.51; N, 7.90. Found: C, 50.03; H, 6.54; N, 8.07. IR (CD₂Cl₂): 2966 (m), 1270 (s) cm⁻¹.

Preparation of *trans*-Bis(di-isopropyl-1-methyl-4-*tert*-butyl-imidazol-2-ylphosphine)₂Pd(CH₃)(NH₂CH₂Ph)[B(Ar_F')₄] ([10c-Me]⁺[B(Ar_F')₄]⁻). Palladium (0) complex **3c** (58.3 mg, 0.095 mmol) was dissolved in benzene (1 mL) to give a clear solution. Iodomethane (13.5 mg, 0.095 mmol) was added with gentle shaking, giving a slightly yellow solution. After 20 min, solvent was removed, and dichloromethane was added to the residue to a homogeneous solution. Benzylamine (10.2 mg, 0.095 mmol) was added to the solution followed by salt, potassium tetra(pentafluorophenyl)borate (67.3 mg, 0.094 mmol). The sequential addition resulted in the formation of a yellow precipitate. After the reaction mixture was filtered through cotton and Celite, the filtrate was concentrated to dryness, and the residue was recrystallized from a diethyl ether/dichloromethane mixture. Yellow crystals were obtained after washing with cold diethyl ether and drying under vacuum (72.7 mg, 46%). Anal. Calcd for C₆₀H₆₆BF₂₀N₅P₂Pd (1415.36): C, 50.88; H, 4.70; N, 4.94. Found: C, 45.26; H, 4.10; N, 4.42. Anal. Calcd for C₆₀H₆₆BF₂₀N₅P₂Pd + 3CH₂Cl₂ (1670.16): C, 45.28; H, 4.34; N, 4.19. IR (CD₂Cl₂): 2967 (m), 1513 (s), 1464 (s) cm⁻¹.

Acknowledgment. D.B.G. and Y.G. thank the U.S. National Science Foundation for partial support under Grant No. 0415783. We thank Grant Boldt and Daniel Lev for initial preparations of phosphines **2a–2c**, and Dr. LeRoy Lafferty for help with advanced NMR experiments.

Supporting Information Available: Molecular structures of **5a-PhBr** and [10c-Me]⁺[B(Ar_F')₄]⁻, CIF files for all structures, and summary of 2D-NMR data used in identification of **3a**, **3c**, and [6a-Me]⁺ OTf⁻. This material is available free of charge via the Internet at <http://pubs.acs.org>.

JA054779U